Physics Department. Annual progress report, 1 January - 31 December 1977

Forskningscenter Risø, Roskilde

Publication date:
1978

Document Version
Publisher's PDF, also known as Version of record

Risø Report No. 374

Risø Report No. 374

Risø National Laboratory

Physics Department
Annual Progress Report

1 January - 31 December 1977

December 1977

Sales distributors: Jul. Gjellerup, Sølvgade 87, DK-1307 Copenhagen K, Denmark
Available on exchange from: Risø Library, Risø National Laboratory, DK-4000 Roskilde, Denmark

December 1977 Risø Report No. 374

Risø National Laboratory

PHYSICS DEPARTMENT
ANNUAL PROGRESS REPORT

1 January - 31 December 1977

edited by
H. Bjerrum Møller and B. Lebech

ISBN 87-550-0513-6

ISSN 0418-6443

PREFACE

Research in the Physics Department at Risø covers three main fields:

Solid-state physics (neutron scattering)
Plasma physics
Meteorology

The principal activities in these fields are presented in this report that covers the period from 1 January to 31 December 1977. Introductions to the work in each of the main fields are given in the respective sections of the report. The contributions marked with § are abstracts of published articles. References to these articles are given in section 5.2.

CONTENTS

[§] Abstract of publication, see also 5.2

§ Abstract of publication, see also 5.2

§ Abstract of publication, see also 5.2

§ Abstract of publication, see also 5.2

1. SOLID STATE PHYSICS

The purpose of the work in solid state physics is to contribute to the fundamental understanding of the physical properties of condensed matter. Neutron beams have properties that make them a unique tool for studies of solids and liquids on the microscopic level. For such investigations use is made of thermal and cold neutrons from the DR 3 reactor, where one double-axis and five triple-axis spectrometers are available. In three of the four tangential through-tubes of the reactor, water scatterers placed close to the reactor core scatter beams of thermal neutrons out through the tube to the spectrometers. The thermal flux in the centre of the beam tube is about $2 \cdot 10^{14}$ neutrons/cm^2/s. A liquid hydrogen cold source was installed in the fourth tangential tube in the spring of 1975. This provides two of the spectrometers with beams of cold neutrons. A curved neutron-conducting tube from the cold source to an experimental hall was installed during the fall of 1977, and one more triple-axis spectrometer is ready for installation in the experimental hall at the end of the flight tube. The possibility of operating a small-angle scattering-instrument at the same site was explored and found feasible. The construction of a further cold source to be installed in the tube next to the present source is in progress, and it is planned to install the source during 1978.

A universal X-ray spectrometer to be used in conjunction with a 12 kW rotating anode X-ray generator or the X-rays produced by a synchrotron is being constructed (1.39-1.40). This is a joint project between Risø National Laboratory and the University of Copenhagen supported by the Danish Natural Science Research Council. In addition, a γ-ray spectrometer suitable for studies of the mosaic distribution in solids is available.

The experimental and theoretical work may be roughly divided into the following main subject fields: investigations of the dynamic and static properties of magnetic (1.1-1.7) and superconducting solids (1.8-1.9); band structure calculations (1.10-1.14); studies of various kinds of phase transitions in magnetic (1.15-1.29) and molecular systems (1.30-1.33); and

investigations of the dynamic and static properties of molecular crystals and adsorbed monolayers (1.34-1.38).

1.1 The magnetism of rare-earth metals§

(A.R. Mackintosh)

Many years of experimental and theoretical investigations of the magnetic structures and excitations in rare-earth metals performed at Risø and elsewhere were reviewed in an article in Physics Today (Mackintosh 1977). The magnetism of rare-earth atoms and the magnetic interactions in crystals were discussed. The way in which these interactions lead to the observed magnetic structures was explained,and the information that may be obtained from the study of the spin wave excitations in heavy rare earths was described. The magnetic properties of the light rare-earths were also discussed, with emphasis on Pr, and the prospects for future research in rare-earth magnetism were briefly considered.

1.2 Excitations and spin waves

(P.-A. Lindgård)

A review of the theory of excitations in strongly anisotropic systems was given (Lindgård 1978a) and illustrated by neutron scattering results on typical systems. When neutron scattering data became available for the light rare earths metals and compounds, a need was felt for a systematic theory for excitations in crystal-field-dominated systems. The crystal field mixes the wavefunctions and provides a coupling between the ground state and the excited states for many operators $(J_x, J_y, J_z \ldots \mathcal{O}_{lm})$, whereas for the Heisenberg system only $\bar{J}$ has a non-zero matrix element to the first excited state. An elegant generalization of the earlier ideas of Trammel (1960) and Grover (1965) was developed simultaneously by several authors. Several examples were given of the successful application of the theory in the interpretation of experiments. The excitation spectrum for neutron scattering is simply given by the poles of the imaginary part of the enhanced wave-vector-dependent susceptibility tensor calculated in the random-phase approximation. A previously unpublished discussion of the effect of two-ion ani-

sotropy was presented (Lindgård 1978a). The formalism reduces to the conventional spin wave theory for the Heisenberg system when the crystal field is negligible compared to the exchange interaction. However, this theory has the drawback that it is

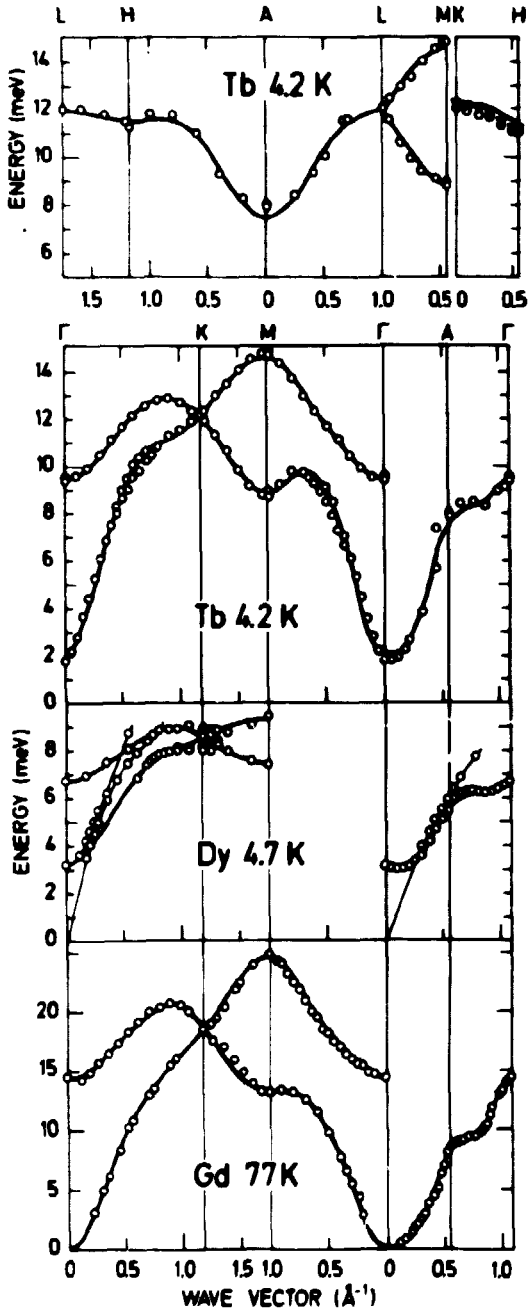

Fig. 1 Dispersion curves for Tb, Dy and Gd, (o). The solid line is the fit to an effective bi-linear Hamiltonian. Qualitative evidence of symmetry-breaking two-ion anisotropy can be found along K-H for Tb and at K for Dy. The thin lines indicate crossing of interacting phonons.

necessary to know the crystal field in advance and each value of J must then be treated separately. For the heavy rare earths, the ratio of the crystal field to the exchange field varies from about 0.2 to about 1 from Tb to Er. Although the ratio is quite large, it is possible to treat the crystal field as anisotropy and express the transverse spin wave relation as a general function of J and with renormalized parameters. However, single-ion anisotropy introduces an effective two-ion anisotropy. A review of the results in the rare-earth Laves-phase compounds and in the heavy rare earths was given, and the status of the current understanding of the interactions in rare earths and their compounds was discussed.

1.3 Spin waves in the heavy rare-earth metals Gd, Tb, Dy, and Er

(P.-A. Lindgård)

The transverse spin wave dispersion relation for strongly anisotropic magnets was formulated in terms of effective renormalized exchange and anisotropy parameters. The spin wave dispersion for the cone structure was considered in detail, including a diagonalization of off-diagonal wave vector dependent terms and renormalization effects caused by the crystal field. The expressions derived require no *a priori* knowledge of the crystal field and magnetoelastic parameters. This is required for the application of the standard basis operator theory. A comprehensive analysis (Fig. 1) of the spin wave data on Gd, Tb, Dy and Er yields the interatomic exchange parameters and the effective anisotropy constants. The exchange parameters obey the de Gennes scaling and decrease as the cubed inverse distance, as expected for the isotropic Rudermann-Kittel interaction. Therefore, there is not much room for an unresolved two-ion anisotropy. The cone spin wave data for Er can be accounted for on the basis of an isotropic exchange interaction, and crystal field parameters with magnitudes in quantitative agreement with those derived from static measurements on dilute Er-Y alloys. No convincing evidence of a giant non-symmetry breaking two-ion anisotropy was found in Tb, Dy and Er. However, evidence of a small symmetry breaking two-ion anisotropy is present in the experimental data.

1.4 Rigorous theory of the spin wave spectrum in a ferromagnet with planar anisotropy

(E. Rastelli and P.-A. Lindgård)

Using the Bose operator expansions derived previously with the matching of matrix element (MME) method (Lindgård and Kowalska 1976) an exact perturbation theory in 1/S was developed of the ground state and the excitation spectrum in a planar ferromagnet. As a preliminary result it was found that the apparent violation of the Goldstone theorem ($E_{q\to 0}\to 0$) for the isotropic Heisenberg Hamiltonian, which is found using the MME or Holstein Primakoff theories in connection with the Hartree-Fock approximation, is resolved when all terms of a given order in 1/S are included in a perturbation theory. The Goldstone theorem is exactly fulfilled, but the spin wave renormalization is no longer simply proportional to the energy. The expansion was carried out to second order in 1/S.

1.5 Theory of rare-earth alloys[§]

(P.-A. Lindgård)

A mean field random alloy theory combined with a simple calculation of the exchange interaction $J(c,Q)$ was shown to quantitatively account for the phase diagrams for alloys of rare-earth metals with Y, Lu, Sc, and other rare-earth metals. A concentration-dependent $J(c,Q)$ explains the empirical "2/3 law", that relates the transition temperature of a rare-earth alloy to the de Gennes factor to the 2/3 power. Thus, a concentration dependent $J(c,Q)$ reconstitutes the idea of de Gennes, who anticipated a linear scaling. The phase diagrams (Fig. 2) exhibit examples of both bicritical and tetracritical points. No significant deviations from the mean-field calculation can be detected with the present experimental accuracy. A linear interpolation of the wavevector dependence of $J(q)$ between Gd and Er is found to account for all alloys except the Sc based alloys. The exceptional behaviour of the Sc alloys is due to a low density of states for Sc. A brief discussion was given of the effect on the mean-field results of changes in volume or c/a ratio and of critical fluctuations. Since the physical mechanisms of these ideal alloys are well documented, they may serve as good candidates for studies of statistical effects such as multicritical phenomena of spin-glass phenomena.

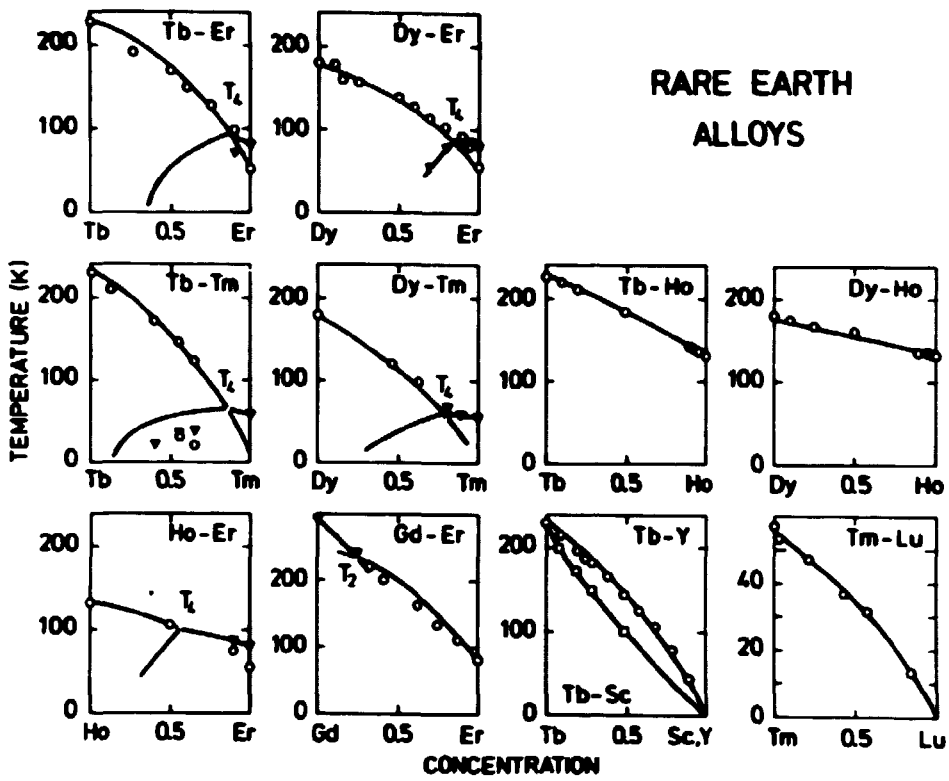

Fig. 2 Phase diagrams for alloys of two different rare-earth metals. The effects of crystal fields are included exactly. The Gd-Er alloys show a bicritical point T_2 and several alloys of elements with competing order parameters show a tetracritical point T_4. The full lines are the calculated phase lines.

1.6 Theory of the temperature dependence of the magnetization in rare-earth - transition-metal alloys§

(B. Szpunar and P.-A. Lindgård)

It was shown that the temperature dependence of the magnetic moments and Curie and ferrimagnetic compensation temperatures for $Gd_{1-x}T_x$ (T = Co, Ni, and Fe) and $Y_{1-x}Co_x$ can be accounted for by a simple model assuming a Rudermann-Kittel-Kasuya-Yosida interaction between the rare-earth moments and the transition-metal pseudo-spin. The interaction is mediated by an effective alloy medium calculated using the coherent potential approximation and elliptic densities of states.

1.7 Temperature dependence of the spin waves in Rb_2CrCl_4

(M.T. Hutchings, J. Als-Nielsen, and P.-A. Lindgård)

Rb_2CrCl_4 is a two-dimensional transparent Heisenberg ferromagnet. The structure of the ferromagnetic planes is nearly a square lattice. However, a small distortion causes the spin structure to be a canted structure with the average moment in the [110] direction. Using one of the cold source triple-axis neutron spectrometers, high precision measurements were made of the spin waves in Rb_2CrCl_4 at energies from 0.01 meV to 10 meV. Further, the renormalization of the spectrum between 5 K and T_c = 52.34 K was studied. A renormalized spin wave theory was developed. The predicted renormalization is in good agreement with that observed. According to the theorem of Mermin and Wagner (1966), no long range order can exist in a two-dimensional Heisenberg magnet. Therefore the q = 0 mode is soft, and we should expect the order and $E_{q=0}$ to disappear at the same temperature. This is confirmed by the spin wave theory and by the experiment.

1.8 Phonons in δ-NbN

(O.W. Dietrich and A. Nørlund Christensen (University of Aarhus))

Most of the transition metal carbides and nitrides have high melting points and show extreme hardness. Some of the compounds are superconductors with high transition temperatures (T ∿ 5-17 K). Measurements of the phonon dispersion curves of several

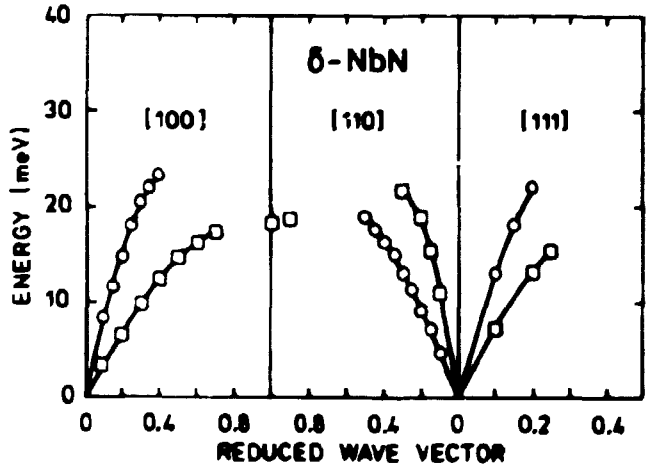

Fig. 3 Phonon dispersion relations of δ-$NbN_{0.95}$. ▫ and ○ are the transversal and longitudinal branches, respectively.

carbides were reported by Smith and Gläser (1970). The superconducting compounds TaC and NbC show anomalies in the acoustic branches, whereas anomalies were not found in the non-superconducting compounds ZrC and HfC. The electronic band structures of the superconducting TiN and ZrN are similar to those of TaC and NbC. Consequently, anomalies are expected and do indeed appear in the phonon dispersion curves of these compounds. Recently, we succeeded in growing a single crystal (0.5 cm^3) of cubic δ-NbN. Stoichiometric δ-NbN has a high superconducting transition temperature, $T_c \sim 18$ K. The crystal we grew has $T_c \sim 12$ K with a composition close to $NbN_{0.95}$. Preliminary measurements of the phonon dispersion relations are shown in Fig. 3. Attempt were made to measure the dispersion relations in the whole Brillouin zone, but above 25 meV the phonon groups broadened and decreased in intensity. Thus there is no evidence yet of anomalies in δ-NbN.

1.9 A reinvestigation of the crystal structure of ε-TaN

(B. Lebech and A. Nørlund Christensen (University of Aarhus))

Tantalum nitride, ε-TaN, was made by annealing of tantalum nitride in nitrogen at 1450°C and 1.4 MPa for 70 h. The crystal structure was determined by powder profile refinement technique using neutron diffraction data. The unit cell is a = 5.196 (4) Å and c = 2.911 (2) Å with three formula units in the cell. The crystal structure of ε-TaN was refined in the space group $P\bar{6}$. The Ta-atoms are closely packed and the distances between them are 2.911 (2) Å (Ta1-Ta1), 3.000 (5) Å (Ta2-Ta3), and 3.334 (5) Å (Ta1-Ta2 or Ta1-Ta3), respectively. The packing of the atoms in the structure is shown in Fig. 4. Ta1 is coordinated with three N-atoms in a planar triangle with the distances Ta1-N = 2.041 (5) Å. Ta2 and Ta3 are coordinated with six N-atoms in a three-sided prism. Here the Ta-N distances are 2.163 (5) Å. The N-atoms are coordinated with five Ta-atoms in a four-sided pyramid with four of the N-Ta interatomic distances equal to 2.163 (5) Å and one equal to 2.041 (5) Å. The structure of ε-TaN described above is different from that determined by Brauer and Zapp (1954) as the N-atom positions are found to be 3j in the space group $P\bar{6}$ instead of 3f in the space group $P6/mmm$.

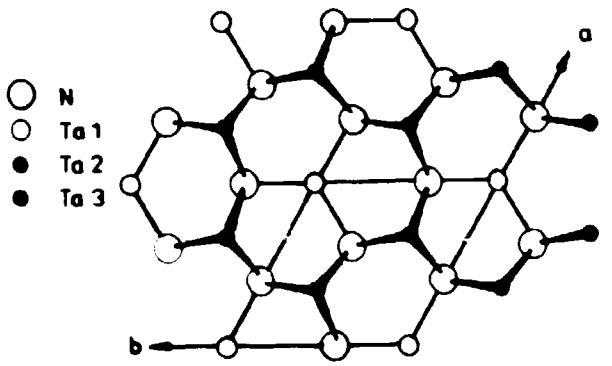

Fig. 4 Projection of the structure of ε-TaN along the [001] direction. Ta-atoms with z = 1/2 are hatched.

1.10 Self-consistent calculation of ground-state properties for ordered transition metal alloys[§]

(H.L. Skriver and O.K. Andersen)

A computationally fast and physically transparent self-consistency procedure based on the atomic sphere approximation of band structure calculations was extended to ordered alloys. Preliminary results were obtained for the equation of state, the equilibrium lattice spacing, the bulk modulus, and the magnetic moments of TiFe, FeNi, and Pd_3Fe.

1.11 Relativistic band structure and Fermi surface of $PdTe_2$ by the LMTO method[§]

(J.-P. Jan (National Research Council of Canada, Ottawa, Canada) and H.L. Skriver)

The energy bands of the trigonal layer compound $PdTe_2$ were calculated, using the relativistic linear muffin-tin orbitals method. The band structure is separated into three distinct regions with low-lying Te 5s bands, conduction bands formed by Pd 4d and Te 5p states, and high-lying bands formed by Pd 5p, Te 6s and Te 5d states. Density of states and joint density of states were calculated from the bands determined over the appropriate irreducible zone. The Fermi surface consists of two closed sheets in bands 11 and 13, and sheets in band 12 connected to one another by tubes. The results allow an explanation of most of the de Haas-van Alphen frequencies observed previously.

1.12 Band structure and Fermi surface of Cu_2Sb by the LMTO method

(J.-P. Jan (National Research Council of Canada, Ottawa, Canada) and H.L. Skriver)[§]

The linear muffin-tin orbital (LMTO) method of band structure calculation was applied to the simple tetragonal compound Cu_2Sb. The d-bands of Cu lie substantially below the Fermi level, and the Fermi surface is a recognizable distortion of the free-electron model. The Fermi surface has sheets in four bands. The first and second bands contain closed sheets, which degenerate along a plane in the absence of spin-orbit splitting. The third band contains a multiply-connected sheet. The fourth band consists of undulating columns, which degenerate along a plane with the third band in the absence of spin-orbit splitting, and of another closed sheet. Earlier de Haas-van Alphen results are explained semi-quantitatively by the model, which also accounts for open orbits seen in high-field magneto-resistance experiments. in the absence of spin-orbit splitting, and of another closed sheet. Earlier de Haas-van Alphen results are explained semi-quantitatively by the model, which also accounts for open orbits seen in high-field magneto-resistance experiments.

1.13 Band structure and optical properties of ordered $AuCu_3$

(H.L. Skriver and H.P. Lengkeek (Kamerlingh Onnes Laboratorium der Rijksuniversiteit Leiden, The Netherlands))

The optical spectra of ordered $AuCu_3$ were measured at low temperatures by a direct ellipsometric technique. We found several structural elements above the absorption edge as well as in the infra-red. The measured spectra are interpreted in terms of the interband absorption calculated from an *ab initio* band structure obtained by the relativistic linear muffin-tin orbital method. The band calculation reveals that ordered $AuCu_3$ has distinct Cu and Au d bands positioned in and hybridizing with an s band common to Cu and Au. The calculated state density is found to be in good agreement with experiment. The Fermi surface is presented and is found to originate mainly in Cu 4s- and 4p states.

1.14 De Haas-van Alphen effect, LMTO band structure and Fermi surface of β'-AgMg

(A.E. Dunsworth*, J.-P. Jan*(* National Research Council of Canada, Ottawa, Canada), and H.L. Skriver)

The de Haas-van Alphen effect was measured in the ordered alloy β'-AgMg. The relativistic LMTO band structure was calculated. It predicts a Fermi surface in good agreement with experiment, and similar to that of other alloys with the same number of conduction electrons per unit cell.

1.15 Phase transitions and critical phenomena

(P.-A. Lindgård)

A review (Lindgård 1978b) was made of studies of phase transitions and critical phenomena in relation to neutron scattering. After a general survey of the fundamentally interesting aspects of this area, the usual concepts, such as order parameter, critical exponents and phase diagrams, were illustrated by a simple example using mean field theory and the Landau expansion. The range of validity of the Landau expansion and the importance of the dimensionality of the lattice (d) and the order parameter (n) were discussed. The effects on phase transitions of competing order parameters and random disorder as well as aspects of the spin-glass phenomena were summarized. The basic principles of the advanced renormalization group theories were outlined. These have provided a breadthrough in the understanding of second-order and perhaps also first order transitions. After a brief account of neutron scattering technique, by means of which one can measure both the response function and the order parameter in many solid state systems, prototypes of experimentally studied systems were discussed. These were classified according to d and n. Also neutron scattering measurements in systems showing multicritical points and spin-glass systems were included. Finally, an outline of possibly interesting and still unexplored areas for future investigations was sketched.

1.16 Mean field theory, the Ginzburg criterion, and marginal dimensionality of phase transitions[§]

(J. Als-Nielsen[+] and R.J. Birgeneau (Massachusetts Institute of Technology, Massachusetts, USA))

By applying a real space version of the Ginzburg criterion, the role of fluctuations and thence the self-consistency of mean field theory can be assessed in a simple fashion for a variety of phase transitions. In using this approach the concept of "marginal dimensionality" emerges in a natural way. For example, for many homogeneous structural transformations, the marginal dimensionality is two, so that mean field theory will be valid for real three-dimensional systems. It was suggested that this simple self-consistent approach to Landau theory should be incorporated in the teaching of elementary phase transition

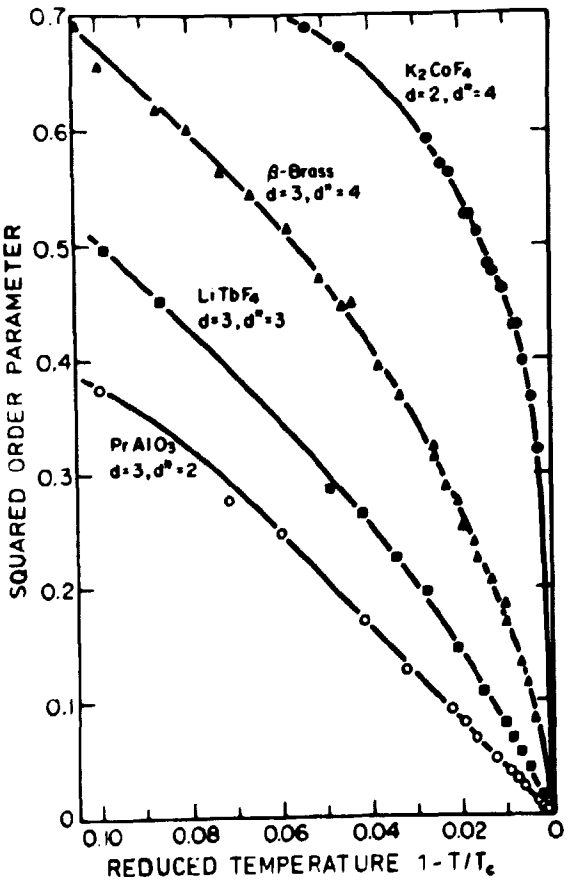

Fig. 5 Squared order parameter, determined by neutron scattering, for the four examples shown in Fig. 6. When the marginal dimensionality $d^* \leq d$, we see Landau behaviour (with logarithmic corrections when $d^* = d$); for $d^* > d$, clear deviations from Landau theory are observed.

[+] Work performed as a guest scientist at Massachusetts Institute of Technology, Massachusetts, USA.

phenomena. The regions of critical fluctuations in direct and reciprocal space of four systems are shown in Fig. 6. The order parameters determined for the same systems are shown in Fig. 5.

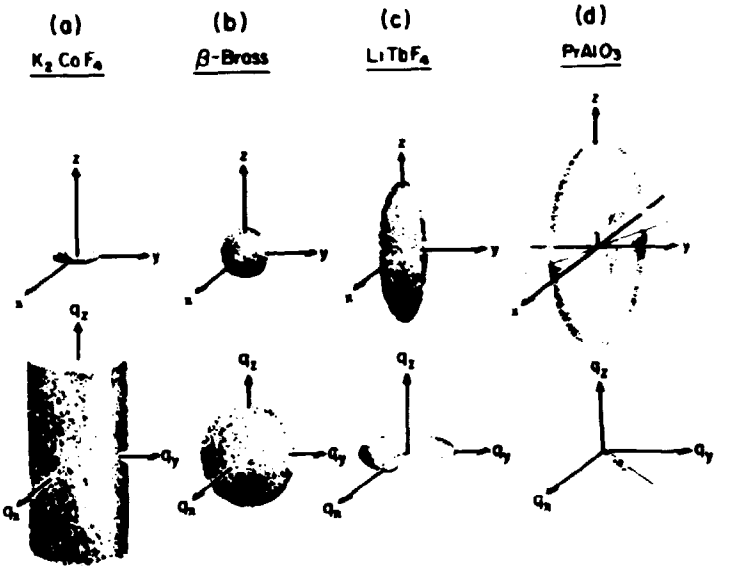

Fig. 6 Regions of critical fluctuations in direct space (top) and in reciprocal space (bottom) for the two-dimensional Ising model (a), the three-dimensional Ising model (b), the dipolar-coupled, uniaxial ferromagnet (c), and for a structural phase transition driven by the softening of an acoustic transverse phonon (d). The dimensions of the regions in direct space enter into the Ginzburg criterion.

1.17 Critical behaviour of pure and site-random two-dimensional antiferromagnets§

(R.J. Birgeneau (Massachusetts Institute of Technology, Massachusetts, and Bell Laboratories, New Jersey, USA),
J. Als-Nielsen+, and G. Shirane (Brookhaven National Laboratory, New York, USA))

Quasi-elastic neutron scattering studies were made of the static critical behaviour in the two-dimensional antiferromagnets K_2NiF_4, K_2MnF_4, and $Rb_2Mn_{0.5}Ni_{0.5}F_4$. For $T < 0.95\ T_N$, the diffuse scattering arises principally from the noncritical transverse susceptibility $\chi^{\perp}(\vec{Q})$. In all three materials, $\chi^{\perp}(\vec{Q})$ is found to

+ Work performed as a guest scientist at Massachusetts Institute of Technology, Massachusetts, USA.

be only weakly temperature dependent for $T < T_N$ with a half-width, $\kappa^{\perp}$, consistent with spin-wave theory. For $|1 - T/T_N| < 0.05$, the overall scattering is dominated by the critical Ising component $\chi''(\vec{Q})$. The total scattering is proportional to $\chi''(\vec{Q}) + \chi^{\perp}(\vec{Q})$ so that, with an appropriate correction for $\chi^{\perp}(\vec{Q})$, the detailed critical behaviour for $\chi''(\vec{Q})$ may be determined. For the reduced temperature range $0.008 < T/T_N - 1 < 0.15$, one finds in all three materials $\nu = 0.9 \pm 0.1$, $\gamma = 1.6 \pm 0.15$, and from the scaling relation $\gamma = \nu(2 - \eta)$, $\eta = 0.2 \pm 0.05$. For $T < T_N$, $\beta = 0.15 \pm 0.015$ in the three systems. Finally, in K_2NiF_4 for $T < T_N$, $\chi^{\perp}(0)$ and $\kappa^{\perp}$ are consistent with two-dimensional Ising behaviour with exponents $\gamma' = 1.75$, $\nu' = 1$; further, $\chi''(+|\varepsilon|) = (50 \pm 10)\chi''(-|\varepsilon|)$ compared with the Ising asymmetry factor of 37. These results hence demonstrate that the site-random and pure systems have identical critical behaviour in agreement with current theory. Moreover, the critical behaviour is close to that of the two-dimensional Ising model, although there are small differences presumably due to the fact that the experiments do not probe the true asymptotic region.

1.18 Investigation of the disorder point

(B. Youngblood, D.P. Landau, and P.-A. Lindgård)

A disorder point is a generalized critical point that occurs in systems with competing interactions (Stephenson 1970). At a temperature higher than the transition temperature between the paramagnetic and the ordered phases, a pseudo transition occurs at which the correlation between next neighbour spins changes sign. Studies of such transitions between different, but incomplete ordered structures are of considerable fundamental interest. An associated phenomenon is the spin-glass transition. For conceptual simplicity, two-dimensional systems are of special interest. Measurements were initiated on $NiCl_2$, which is an example of such a system, but the interpretation of these preliminary results is uncertain. A molecular dynamics calculation shows clearly the change of sign for a two-dimensional system. Work on high temperature expansion theory was initiated to account for this effect.

1.19 Determination of the critical exponent β in the Ising magnet $MnNb_2O_6$

(K Nørgaard Clausen and B. Lebech)

$MnNb_2O_6$ has the orthorhombic columbite structure with four formula units per unit cell. The Mn^{3+} ions are magnetic, and order at $T_N \sim 4.42$ K in an antiferromagnetic structure described by Nielsen et al. (1976). The transition at T_N is of second order. A preliminary analysis (Fig. 7) of the (1,2,0) Bragg

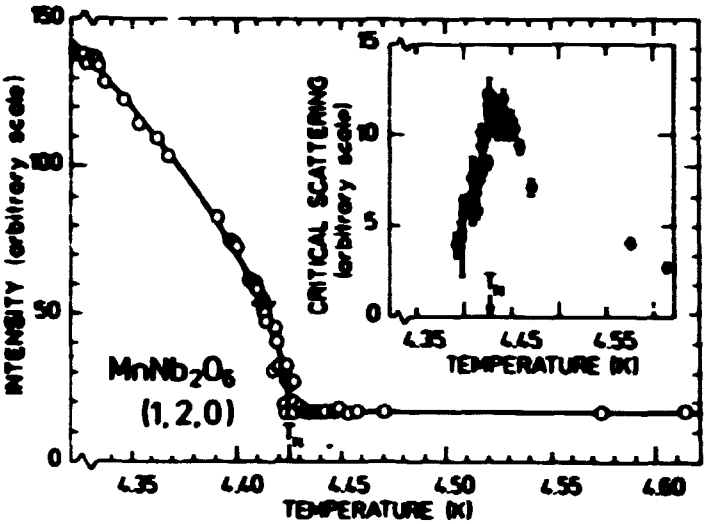

Fig. 7 Intensity of the (1,2,0) Bragg peak in $MnNb_2O_6$ after subtraction of the critical scattering near T_N. The intensity above T_N originates from the (1,2,0) nuclear Bragg peak. The estimated critical scattering is shown in the inset.

intensity near T_N results, after a crude correction for the critical scattering, in a critical exponent $\beta = 0.30 \pm 0.02$. This value of β is in good agreement with the value of β obtained from renormalization group theory (Mukamel et al. 1976) for a d = 3, n = 1 system. An attempt to make a more accurate correction for the critical scattering is in progress.

1.20 Critical behaviour of the magnetization in TbSb and $Tb_{0.6}Y_{0.4}Sb$

(K. Carneiro, N. Hessel Andersen (University of Copenhagen), J.K. Kjems, and O. Vogt (ETH, Zürich, Switzerland))

Neutron elastic scattering was used to study the temperature dependence of the sublattice magnetization in TbSb and

$Tb_{0.6}Y_{0.4}Sb$. The transition from a type II antiferromagnet into a paramagnet is found to be continuous in both cases. This does not support the recent theoretical prediction that the transition in TbSb should be of first order (Bak et al. 1976). since the Hamiltonian shows no stable fixed point within the ε-expansion. In pure TbSb, we find the critical exponent $\beta = 0.20 \pm 0.01$ in the region $4 \cdot 10^{-3} < (T_N - T)/T_N < 2 \cdot 10^{-1}$. In $Tb_{0.6}Y_{0.4}Sb$, the exponent is significantly different. We find a sharp transition with $\beta = 0.37 \pm 0.05$.

1.21 The magnetic phase diagram of the anomalous antiferromagnet CeSb

(B. Lebech, P. Fischer*, B.D. Rainford (Imperial College, London, U.K.), G. Meier* (* ETHZ, Wurenlingen, Switzerland), and O. Vogt (ETH, Zürich, Switzerland))

The magnetic ordering of the anomalous antiferromagnet CeSb, which has a NaCl crystal structure, was determined in zero and non-zero magnetic fields applied parallel to the [001] and [011] directions ($H < 5T$) by means of neutron diffraction investigations of single crystals and powder.

Below the Néel temperature of (16.1 ± 0.1) K, in zero field, there are six partially disordered magnetic phases of antiphase-domain type (<100> superstructures) with <100> orientation of the magnetic moments. At 4.4 K, the ordered magnetic moment equals (2.10 ± 0.04) μ_B, which corresponds to the free ion value of 2.14 μ_B for Ce^{+3}. The temperature dependence of the ordered moment shows a first-order phase transition at T_N. At approximately $T_N/2$ there is a first-order phase transition to a f.c.c. type IA low temperature configuration. All these antiferromagnetic structures may be described in terms of four simple, stacked blocks composed of ferromagnetically ordered or completely disordered layers of Ce^{3+} moments. Two of these blocks consist of two ferromagnetic layers each that are ferromagnetically coupled (F_+; F_- or ++; --). Each of the two other blocks consists of one disordered layer sandwiched between two antiferromagnetically coupled ferromagnetic Ce^{3+} layers (D_+; D_- or +0-; -0+). The high-temperature structure in zero-applied magnetic field is D_- (Fig. 8b), while the low-temperature

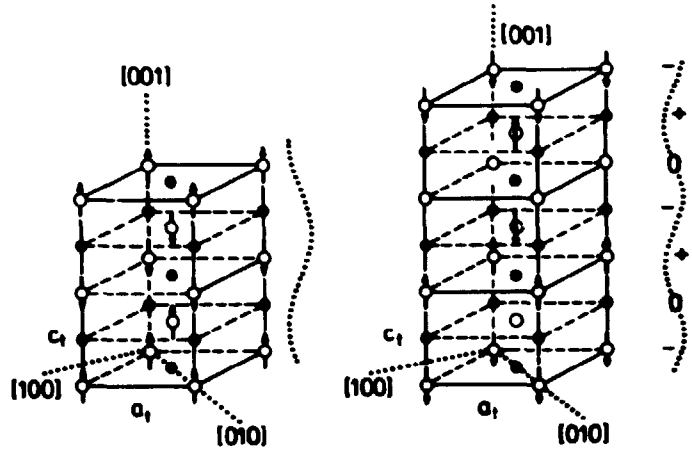

Fig. 8 Basic antiferromagnetic structures of CeSb corresponding to phases VI (F_+F_-) and I (D_-) (Z-domains). The tetragonal magnetic unit cells are shown. o Ce-atoms, • Sb-atoms.

structure was found to be a type IA (or F_+F_-) (Fig. 8a) antiferromagnet. Although all the magnetic structures of CeSb in zero-applied magnetic field are adequately described by the stacking sequence, each structure may formally be represented in terms of finite Fourier series by Fourier components parallel to the <100> axes. The Fourier components corresponding to F_+F_- and D_- are also shown in Fig. 8.

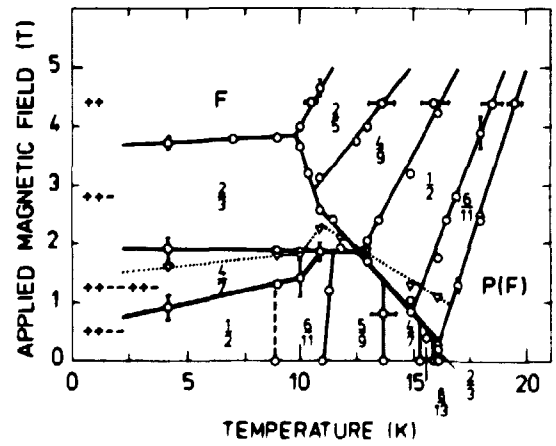

Fig. 9 Magnetic phase diagram of CeSb for magnetic fields $\vec{H}$ applied parallel to [001]. The positions (Q) of the most intense magnetic satellites are marked on the diagram. The error bars indicate predominantly hysteresis effects. The heavy line indicates the borderline between the low field antiferromagnetic phases and the high field metamagnetic phases. At fields above the dotted line only a single Z domain persists.

At low temperatures and increasing magnetic fields, the structures transform from antiferromagnetic via ferrimagnetic configurations to a ferromagnetic state, i.e. the magnetic properties are similar to those of Ising spins. At higher temperatures ($T > 10$ K) the existence of antiphase-domain-type superstructures along the tetragonal c-axis implies considerable disorder even at high fields, and partially ordered, field-induced states exist even above the Néel temperature in zero field. The magnetic phase diagram is shown in Fig. 9.

The change from a first-order transition at the Néel temperature in zero field to a second-order transition at high fields points to the existence of a tri-critical point, presumably at $T \sim 16$ K and $H \lesssim 0.3$ T.

1.22 Commensurable to incommensurable transition in the magnetic-spiral-phase of 90% Ho-10% Tb

(J.D. Axe, J.K. Kjems, and B. Lebech)

The magnetic order in 90% Ho-10% Tb that sets in at $T_N = 145$ K is characterized by a spiral wavevector Q along the c-axis. The pitch of the spiral changes gradually from about 40° turn angle per layer at T_N to about 33° per layer at about 40 K, where a more rapid change with temperature begins until a commensurable structure with 30° per layer appears at 30 K. Upon further cooling, a first-order transition to a basal plane ferromagnetic state takes place at 20 K. We have studied in detail the temperature dependence of the spiral wave vector in the temperature range 20 to 65 K. In order to obtain the highest precision, the magnitude of Q was deduced from the separation between the (0,0,0+5Q), (0,0,0+7Q), 0,0,2-5Q) and (0,0,2-7Q) Bragg multiplex around the (0,0,1) reciprocal lattice point. It was found that the commensurable to incommensurable transition at 30 K is almost continuous but that it shows considerable hysteresis ($\sim$ 3 K). In the transition region both phases appear simultaneously in the diffraction patterns. Formally, the transitions may be treated by the theory that was developed for the commensurable to incommensurable structural transition in $TaSe_2$ by McMillan (1975). In this case the result is two coupled non-linear wave-equations for the equilibrium structure that can be decoupled and solved analytically. Qualitatively, the observed variation

of Q with temperature follows the theoretical prediction except for the hysteresis.

Also the excitation spectrum was examined, and in the commensurable phase, a spin wave energy gap of 0.5 meV was found at the commensurable wave vector position. The gap energy decreases slightly as the temperature approaches the transition at 30 K, but a more pronounced effect is the increased damping of the spin wave modes at small wave vectors. Above 30 K, only overdamped spectra are observed up to half the zone boundary. This behaviour was also found in pure Ho but it is in marked contrast to the findings in the spiral phase of pure Tb, where well defined spin waves are observed at small wave vectors up to $T_N \sim 224$ K.

1.23 Magnetic structures and phase transitions of Nd

(B. Lebech and P.Å. Hansen)

The magnetic structure of dhcp Nd was first investigated by Moon et al. (1964), who suggested a structural model in which the spins at the hexagonal sites order below 20 K in a modulated antiferromagnetic structure, and in which the spins at the cubic sites order below 7.5 K in a similar way. However, it was pointed out (Moon et al. 1964) that the proposed model failed to describe all the observed diffraction effects. This was further corroborated by recent neutron scattering experiments, Lebech and Rainford (1974), S.A. Shapiro and S. Sinha (private communication). In an attempt to finally determine the magnetic structure of Nd, a set of magnetic intensities was measured on a single crystal sphere of diameter 2 mm at 11 K, i.e. well above the transition at 7.5 K. The results agree qualitatively with results obtained on a much larger cylindrical crystal (6 mm diameter, 10 mm long), although the results obtained with the large crystal are affected by extinction. The measured intensities were analyzed in terms of a general model having 15 independent parameters. In this model the moments $\vec{S}_{\ell\nu}$ at each site (hexagonal or cubic) are given by

$$\vec{S}_{\ell\nu} = \vec{A}_\nu \exp(+i\vec{Q}_n \cdot (\vec{R}_\ell + \vec{d}_\nu)) + \vec{A}_\nu^* \exp(-i\vec{Q}_n \cdot (\vec{R}_\ell + \vec{d}_\nu)), \qquad (1)$$

where ℓ labels the unit cell and ν the atom within the unit cell.

The modulation vector $\bar{Q}_n$ is determined from the appearance of the magnetic superlattice peaks that lie along equivalent $\hat{b}_1$ directions. Above 7.5 K, $Q_n \sim 0.12$, while two sets of modulation vectors coexist below 7.5 K ($Q_n \sim 0.12$ and $Q_m \sim 0.18$).

The elastic magnetic cross-section calculated for the general model (1) agrees with the diffraction effects observed at 11 K. Another set of intensities measured at 4.2 K, i.e. well below the transition at 7.5, is also being analyzed by means of equation (1). The intensities of equivalent $(Q_n,0,3)$ magnetic satellites were found to decrease almost linearly with increasing temperature from 16 K to T_N (Fig. 10). From a least squares

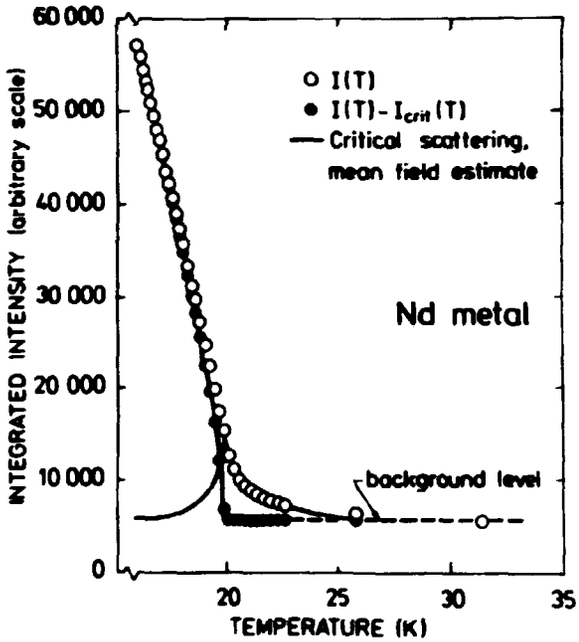

Fig. 10 Temperature dependence of the magnetic $(Q_n,0,3)$ satellite intensity of Nd before (o) and after (•) subtraction of a mean field estimate of the critical scattering. The line through the filled circles is the result of a least squares fit to a power law giving T_N = (19.9±0.1), K and β = (0.36±0.02).

fit of the measured intensities to $I(T) = C(1-T/T_N)^{2\beta}$ we found after subtraction of a mean field estimate of the critical scattering below T_N, β = (0.36 ± 0.02) and T_N = (19.9 ± 0.1) K. Based on renormalization group theory and the ε-expansion, Mukamel et al. (1976) predicted $\beta_\varepsilon \sim 0.38$ for Nd, assuming that the Moon model describing the magnetic structure is correct. However, as the structure described by (1) and the Moon model

belong to the same universality class they should have the same value of β_ε. Thus the value of β deduced from these measurements agrees with β predicted by the ε-expansion.

1.24 Field-dependent magnetic phase transitions in mixed-valent TmSe[§]

(H. Bjerrum Møller[+], S.M. Shapiro (Brookhaven National Laboratory, New York, USA), and R.J. Birgeneau (Massachusetts Institute of Technology, Massachusetts, USA))

A neutron diffraction study of the field-dependent magnetic ordering in TmSe showed that the magnetic structure in zero fields is antiferromagnetic fcc type I with T_N = 3.2 K. The magnetic phase diagram may be understood as a successive domain reorientation and metamagnetic transitions for T < 3 K with increasing field. This can be explained quantitatively by using a simple classical spin Hamiltonian. The mixed-valent character manifests itself mainly in a reduced moment and in a markedly altered crystal field.

1.25 Effect of hydrostatic pressure on the critical fluctuations in the induced moment system Pr_3Tl

(J.K. Kjems, M. Nielsen, and W.J.L. Buyers (Chalk River, Nuclear Laboratories, Canada))

Pr_3Tl orders at 11.2 K at atmospheric pressure. Guertin et al. (1977) showed that hydrostatic pressure lowers the ferromagnetic transition by as much as 1.5 K/kbar. Previous studies have shown that the critical fluctuations give rise to a strong elastic component in the forward scattering from a polycrystalline sample of Pr_3Tl, and the purpose of the present experiment was to study the temperature and pressure dependence of this scattering in order to shed light on the microscopic origin of this feature. The experiment was carried out with a 2 cm^2 Pr_3Tl sample placed in a Al-pressure cell in which the hydrostatic pressure was supplied by ^4He via a capillary tube. The maximum pressure for this set-up is 4 kbar at 4 K. Figure 11 shows the temperature-dependence of the integrated Bragg intensity of the

---

+ Work performed as a guest scientist at Brookhaven National Laboratory, New York, USA.

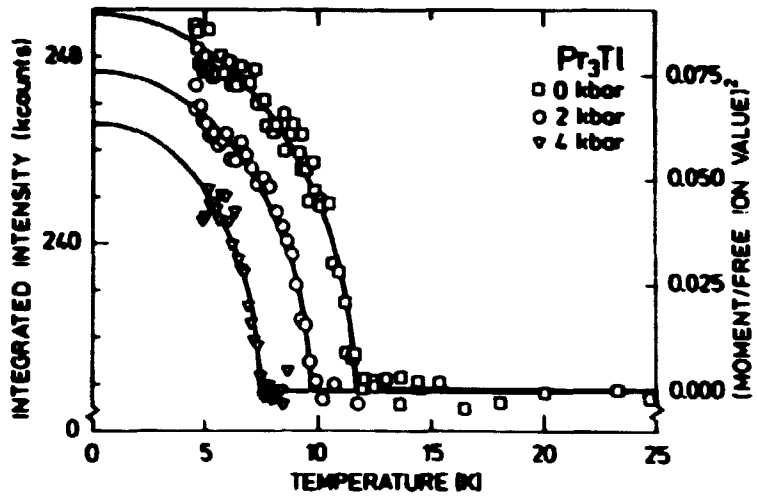

Fig. 11 Temperature dependence of the integrated (1,1,1) intensity from a polycrystalline sample of Pr_3Tl for three different hydrostatic pressures. The full lines represent least squares fits which are used to derive the Curie temperature and the saturation magnetization at each pressure.

(1,1,1) powder peak for three different pressures. From these data, we have derived the pressure dependence of the Curie temperature and the saturation magnetization. The critical scattering is also dramatically altered by the pressure. Temperature scans at fixed momentum transfer near the forward beam show decreasing intensity and less pronounced peaking at T_c with increasing pressure. All intensities are normalized using the (1,1,1) nuclear powder intensity and the critical scattering is found to be much stronger than predicted by the random phase approximation theories previously used to analyse Pr_3Tl data.

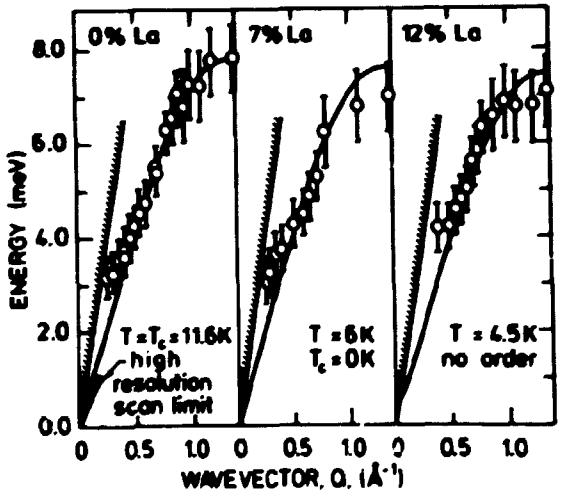

Fig. 12 The observed dispersion of the Γ_1-Γ_4 exciton in $(Pr_{1-x}La_x)_3Tl$. The cross-hatched line indicates the kinematic restriction in the experiment. Also shown is the region of the high-resolution long-wavelength scans in which a central mode is observed. The full curves are the results of random phase approximation calculations.

1.26 Observation of a central mode in an exchange-coupled singlet-ground-state system[§]

(J. Als-Nielsen, J.K. Kjems, W.J.L. Buyers (Chalk River, Nuclear Laboratories, Canada), and R.J. Birgeneau (Massachusetts Institute of Technology, Massachusetts, USA))

A central mode in the ferromagnetic phase transition of Pr_3Tl was observed by inelastic and quasielastic neutron scattering. The integrated intensity has a Lorentzian wave vector dependence with a correlation range that is much larger than in ordinary ferromagnets. The softening of the exciton mode is considerably smaller than predicted by mean field theory. Figure 12 shows the observed dispersion of the $\Gamma_1 - \Gamma_4$ exciton in $(Pr_{1-x}La_x)_3Tl$.

1.27 Cooperative Jahn-Teller transition in the metallic system $PrCu_2$

(J.K. Kjems, H.R. Ott (ETH, Zürich, Switzerland), S.M. Shapiro (Brookhaven National Laboratory, New York, USA), and K. Andres (Bell Laboratories, New Jersey, USA))

Bulk measurements of, e.g., heat capacity, susceptibility, resistance, and thermal expansion have indicated that $PrCu_2$ undergoes a structural transition at 7.25 K, which is driven by the cooperative Jahn-Teller effect. We have studied this transition using both elastic and inelastic neutron scattering and our main findings are:

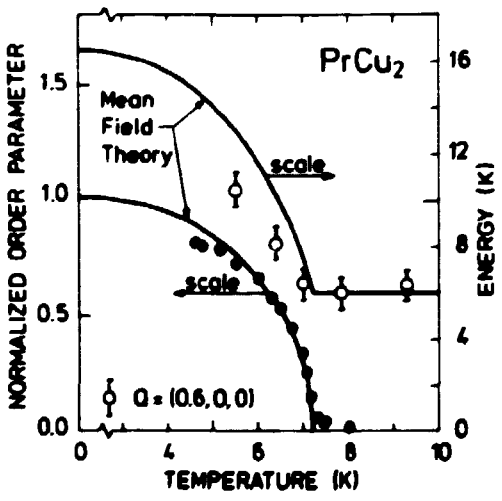

Fig. 13 Temperature dependence of the reduced strain order parameter (e) and of the energy of the weak crystal field excitation at (0.6,0,0) between the lowest two singlets in $PrCu_2$, near the Jahn-Teller transition at 7.25 K.

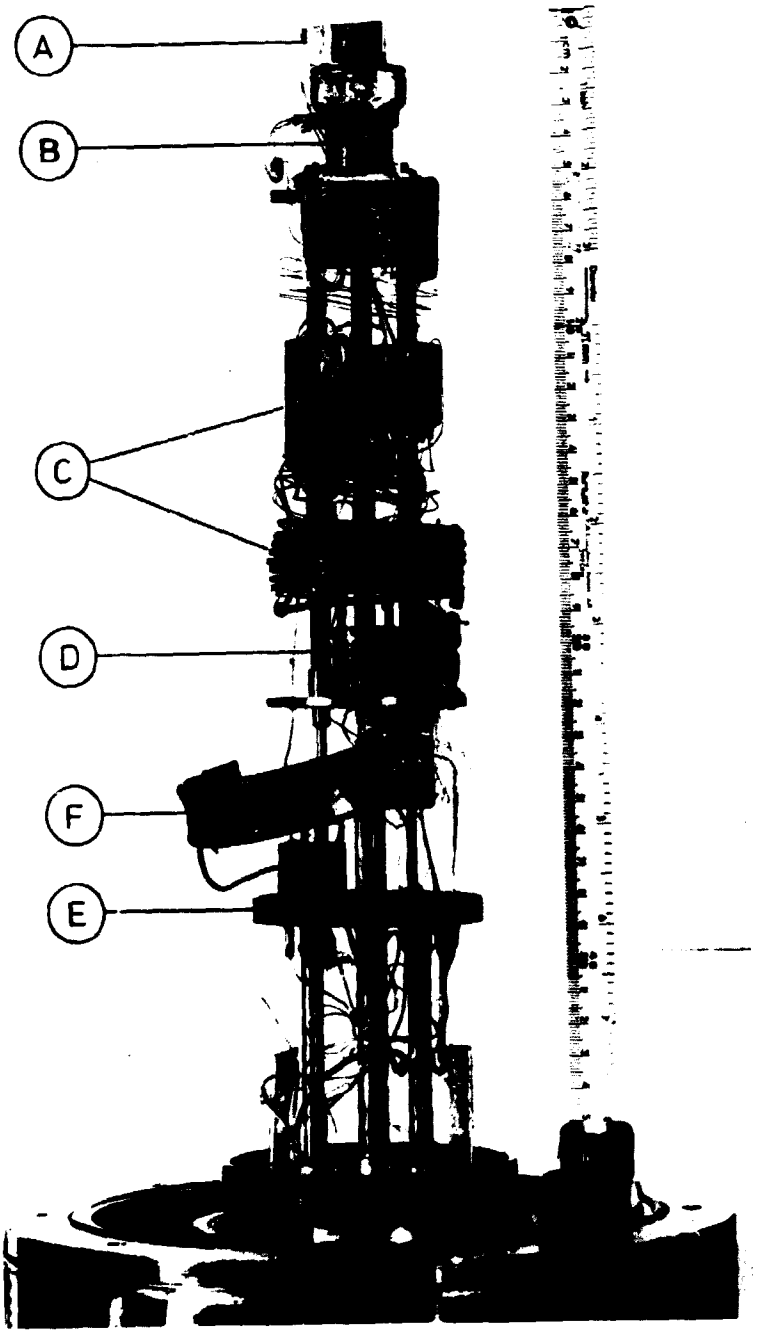

Fig. 14 $^{3}He/^{4}He$ dilution refrigerator for neutron scattering experiments. The refrigerator (D) is built on to the bottom flange of a standard 4 l He dewar and the cryostat fits the goniometers on the spectrometers. By means of this refrigerator, measurements can be performed with the sample at temperatures down to 25 mk. (A) Al-container inside which a single crystalline sample is mounted. (B) Mixing chamber with electrical wires for thermometers and heater. (C) Heat exchangers. (D) Still. (E) Flange, cooled by pumped ^{4}He. (F) Cooling spiral used for cooling down to 4.2 K.

1. The structural change at 7.25 K alters the symmetry from orthorhombic to monoclinic and it involves a shear distortion in the a-c plane. The point symmetry at the Pr^{+3} sites is C_{2v} in the high temperature phase and the symmetry breaking distortion belongs to the B_1 representation.
2. The temperature dependence of the order parameter was measured via the strain in the a-c plane, as the difference between $|\tau_{101}|$ and $|\tau_{10\bar{1}}|$. Figure 13 shows the normalized results compared with a mean field theory. From the measurement of the elastic constants at room temperature, and from the observed low temperature distortion, we deduce that the strength of the coupling between the Pr^{+3} ions, due to the homogeneous strain, amounts to 5 K per ion. The total interaction strength is 8.5 K/ion as determined from the observed crystal field splitting between the two lowest levels above T_D and the observed T_D.
3. A weakly temperature-dependent crystal field excitation is observed with the momentum transfer along the crystallographic a-axis. The symmetry of this excitation is the same as the observed distortion at low temperature, and we identify this electronic mode as the driving force of the Jahn-Teller effect. The energy versus temperature dependence of this excitation at (0.6,0,0) is shown in Fig. 13, again compared to mean field theory.
4. A strong magnetic dipole transition was observed with the momentum transfer along the b and c axes of the crystal. The observed dispersion shows that the magnetic interactions would favour an antiferromagnetic magnetic ordering, which is consistent with the suggested combined nuclear and electronic magnetic ordering at 54 mK. It is planned to study this magnetic transition further using the dilution refrigerator, (Fig. 14), which now has become operational.

1.28 γ-ray diffraction studies of the mosaic distribution in $TmAsO_4$ near the cooperative Jahn-Teller transition at 6 K

(K. Møllenbach, J.K. Kjems, and S.H. Smith (Oxford University, U.K.))

In a number of rare-earth vanadates and arsenates a structural phase transition from a tetragonal to an orthorhombic structure takes place at low temperatures. The transition is a cooperative

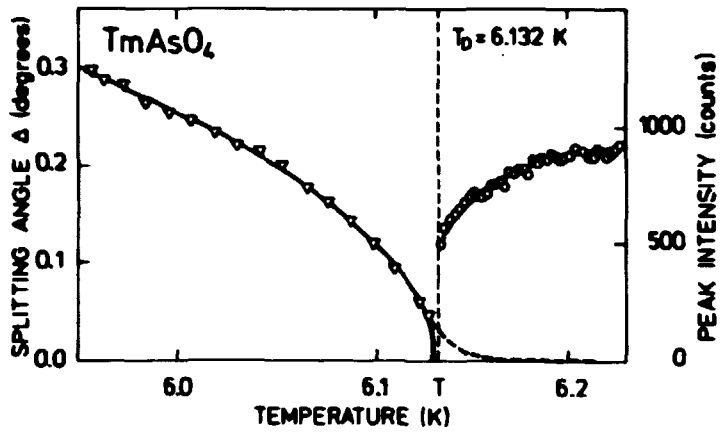

Fig.15 Left side: The splitting angle of the (2,0,0) mosaic distribution as a function of temperature (▽). Right side: The peak intensity of the (2,0,0) reflection above T_D (o). The dashed line at the bottom indicates the precursor changes in the observed width.

Jahn-Teller transition driven by the coupling of the electronic E-doublet of the tetragonal phase to the B_{2g} strain (in the Tb and Tm compounds) or the B_{1g} strain (in the Dy compounds). As the orthorhombic distortion develops, a twinning pattern evolves which gives rise to a splitting of the mosaic distribution of the (2,0,0)-Bragg reflection (B_{2g} strain), or of the (2,2,0)-Bragg reflection (B_{1g} strain).

This type of phase transition was studied using γ-ray diffraction. So far, a precise measurement of the critical exponent, β, in $TmAsO_4$ confirms the earlier reported classical value of $\beta = 0.50 \pm 0.03$. More interestingly, we observe precursor effects in the mosaic distribution as T_D is approached from above (see Fig. 15).

1.29 Neutron scattering from magnetic domains in $LiTbF_4$

(K. Møllenbach, J.K. Kjems, J. Als-Nielsen, and I. Laursen (Technical University of Denmark))

The study of neutron scattering from magnetic domains in the dipolar-coupled Ising ferromagnet $LiTbF_4$ was continued. Data were collected in two regions of reciprocal space: 1) $0.0005\ \text{Å}^{-1} < |\bar{q}| < 0.01$ and 2) $0.01 < |\bar{q}| < 0.07\ \text{Å}^{-1}$, $\bar{q}$ being the momentum transfer vector.

The measurements in the small $|\bar{q}|$ region were made using a triple-axis spectrometer modified to an extreme resolution by employing perfect Si-crystals as effective collimators before and after the sample. The intensity profiles obtained in this way are strongly affected by neutron-optical effects, i.e. refraction and total reflection at domain boundaries. Monte Carlo simulation is being used to gain understanding of this phenomenon. The large $|\bar{q}|$ region is accessible with a double-axis spectrometer using ordinary Soller collimators. The data from this region gives the following picture of the domains:
The magnetic domains are elongated objects described by two characteristic lengths: $\kappa_{||}$ along and $\kappa_{\perp}$ perpendicular to the Ising-axis (z-axis) with $\kappa_{||} > \kappa_{\perp}$. The domains are surrounded by domain walls with a characteristic width λ. Scaling allows the data to be mapped on one and the same curve suggesting that $\kappa_{||}$, $\kappa_{\perp}$ and λ are coupled to the correlation length of the system near T_c. Furthermore, the measurements show that the correlations are stronger along the Ising-axis than perpendicular to the Ising axis.

1.30 Structural phase transition of octafluoronaphthalene

(G.A. Mackenzie, B. Buras, G.S. Pawley (University of Edinburgh, Scotland))

Octafluoronaphthalene undergoes a structural phase transition to Phase II at 266.5 K at atmospheric pressure. Both the high and the low temperature structures are monoclinic $P2_1/c$ with two and four molecules in the unit cell, respectively. The nature of this phase transition was the subject of a single crystal neutron diffraction study (Pawley and Dietrich 1975) and a neutron powder diffraction and Raman scattering study (Mackenzie et al. 1977).

A similar phase transition has now been discovered at about 1 kbar at room temperature by neutron powder diffraction. The data were obtained using the large volume high-pressure cell that allows conventional 2θ scans at pressures up to about 8 kbar (Buras et al. 1977). Powder diffraction patterns at various pressures were recorded using a triple axis spectrometer in the elastic mode at a wavelength of 2.38 Å equipped with pyrolytic graphite monochromator, analyser, and filter.

The data were analysed using the profile refinement program EDINP (Pawley, Mackenzie, and Dietrich 1977) with the atom positions constrained to preserve the molecular shape. Good fits were obtained for scans measured at 2 kbar and 4 kbar, both with R-factors of ∿ 12%. Observed and calculated profiles for the 2 kbar are shown in Fig. 16. The results confirmed that the structure at pressures above 0.8 kbar is very similar to that below 266.5 K at atmospheric pressure.

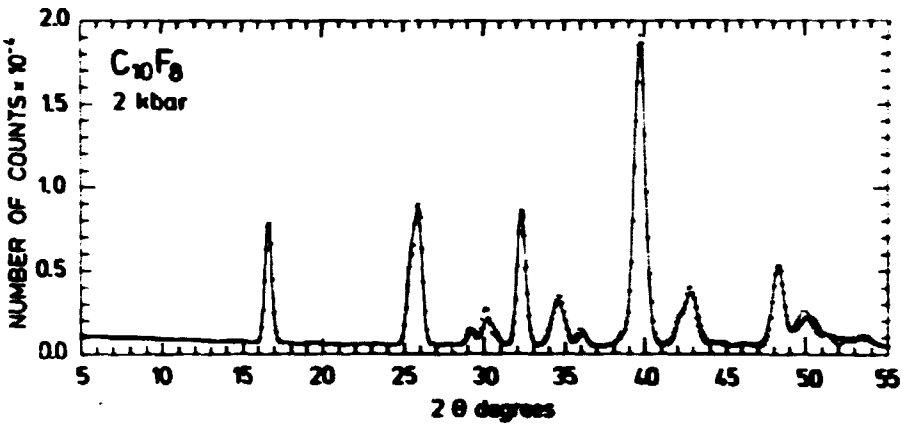

Fig.16 Observed and calculated neutron diffraction pattern of octafluoronaphthalene at room temperature and 2 kbar.

Evidence of a further structural change was found at pressures of 6 kbar and above. Several weak features appeared in the pattern and these could not be indexed according to the Phase II unit cell. Scans at higher pressure using the fixed scattering angle pressure cell (Buras et al. 1977) showed that one of these peaks increases considerably in intensity as the pressure is increased. A likely explanation of this is that there is a distortion in the structure which sets in at between 4 and 6 kbar, causing a unit cell doubling along either the b or the c direction. No attempt was made to refine the structure of this new phase because the data available are insufficient to permit the use of the increased number of variable parameters, which results from the loss of symmetry between the molecules in the unit cell.

1.31 Phase transition in solid pyrene

(G.A. Mackenzie, B. Buras and R. Berg (Technical University of Denmark))

Pyrene, $C_{16}H_{10}$, is an aromatic molecular crystal with a monoclinic $P2_1/a$ structure at room temperature and atmospheric pressure (Phase I) (Hazell et al. 1972). It has been known for some time that the material undergoes a phase transition at low temperature but the structure of the low temperature form is as yet unknown. Recently light scattering measurements have shown that dramatic changes in the phonon spectra occur at high pressure (4 kbar, 300 K) as well as at low temperature (1 bar, 110 K) (Zallen et al. 1976). The similarities in the high pressure and low temperature spectra suggest that the crystal structure is the same in both cases (Phase II). Structure determination of Phase II by conventional single crystal techniques is not possible because the crystal shatters on going through the transition. Neutron powder diffraction however offers the possibility of obtaining reliable structural data at low temperatures and high pressures and the data may be analyzed using the profile refinement program. Although the refinement program is primarily designed to obtain better information on an already approximately known structure, it can be used to solve unknown molecular crystal structures (Pawley, Mackenzie, and Dietrich 1977).

Recently, we measured neutron powder diffraction patterns from a 98% deuterated sample, $C_{16}D_{10}$, at low temperatures. Surprisingly, there was no clear evidence of a phase transition occurring at low temperature, the pattern measured at 5 K appearing similar to that measured at room temperature. Both sets of data were fitted using the same model structure, Phase I, and gave equally good refinements, R = 9.4% and 7.7%, respectively. The slightly better fit at 5 K is due to the decrease in the thermal motion. Although the refinements suggest that the structure remains Phase I down to 5 K, there is slight evidence of a deviation from this structure. At room temperature, diffraction patterns were measured at 2, 4 and 6 kbar using the large volume high pressure cell (Buras et al. 1977). The 2 and 4 kbar patterns showed very little deviation from the atmospheric pressure pattern. The 6 kbar pattern, on the other hand, developed over a period of a few days into a pattern totally different from that at atmospheric pressure.

The 2 and 4 kbar patterns showed similar differences from the calculated Phase I profiles as observed in the 5 K patterns. It is interesting to note that these weak features occur where strong peaks develop at 6 kbar, indicating that the structural change may be under way at 5 K and at 2 and 4 kbar. The structure of Phase II has not yet been solved, but we have a reliable set of data at 6 kbar that can be used for this purpose.

It is not clear why the neutron diffraction study gives a picture of the phase transition different from that found in the light scattering study. The time dependence of the phase transition was only observed in the neutron scattering data, and it seems unlikely that the difference between $C_{16}H_{10}$ and $C_{16}D_{10}$ could lead to such a difference. However, we are currently investigating both materials by infrared and Raman spectroscopy and hope to gain more insight into this interesting phase transition.

1.32 High-resolution X-ray study of a second-order nematic to smetic-A phase transition §

(J. Als-Nielsen[+], R.J. Birgeneau[*], M. Kaplan[*], J.D. Litster[*], and C.R. Safinya[*], ([*]Massachusetts Institute of Technology, Massachusetts, USA))

A high-resolution X-ray-scattering study was made of the critical fluctuations in the nematic phase associated with the nematic to smectic-A transition in N-p-cyanobenzylidene-p-octyloxy-anilene (CBOOA). For $8 \cdot 10^{-5} \lesssim T/T_c - 1 < 2 \cdot 10^{-2}$, the transverse and longitudinal correlation lengths were found to diverge with identical exponents, that is, $|\nu_L - \nu_T| < 0.03$. As T_c is approached, the system appears to cross over from helium-like to mean-field critical behaviour at a reduced temperature of $\sim 10^{-3}$. The data shown in Fig. 17 were fitted to a cross section of the form (with $\vec{q} \equiv \vec{k}_i - \vec{k}_f$)

$$\sigma(\vec{q}) = \frac{a\xi^2}{1+[\xi(q_{||}-q_o)]^2+[b\xi q_\perp]^2+c[b\xi q_\perp]^4} \qquad (2)$$

convoluted with the instrumental-resolution function. For this

---

+ Work performed as a guest scientist at Massachusetts Institute of Technology, Massachusetts, USA.

cross section, the susceptibility was $\sigma(q_o) = a\xi^2$, the longitudinal correlation length $\xi_L = \xi$, and the transverse correlation length $\xi_T = b\xi$.

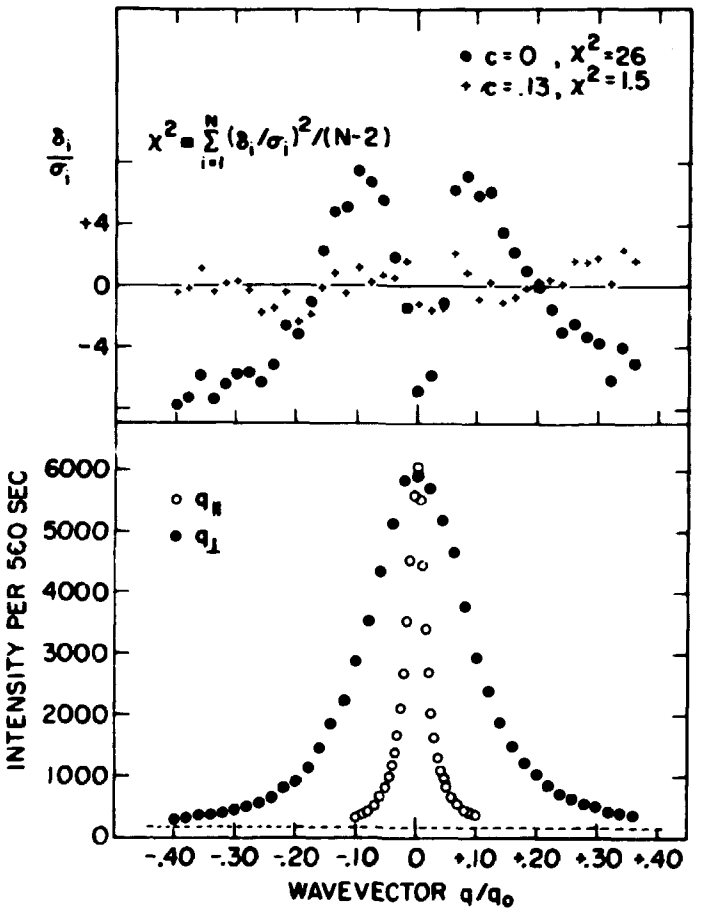

Fig. 17 Lower panel: transverse and longitudinal scans at $T/T_c = 0.0052$; upper panel: deviations for the best of fits of equation 2 (1.17) to the transverse scan with the fourth-order term fixed at c=0 and allowed to vary as a free parameter (c=0.13).

1.33 Hydrodynamic instabilities and neutron scattering

(T. Riste*, K. Otnes* (* IFA, Kjeller, Norway), and H. Bjerrum Møller)

The flow pattern in a liquid layer heated from underneath changes character as the vertical temperature gradient is increased. Utilizing the coupling that exists between the molecular orientation and the flow in a liquid crystal, neutron scattering was used to explore these phenomena. Experiments

near the lowest-lying instability, the Rayleigh-Bénard transition, verify the mean-field predictions for the change of the threshold gradient with the applied magnetic field, the behaviour of the order parameter (the fluid velocity) versus ε (the reduced gradient scale), the time-dependent growth and the critical slowing-down of the growth-rate of the order parameter.

A pretransitional tail of intensity was analyzed within the same formalism and it was suggested that the tail arises from hydrodynamic fluctuations driven by the microscopic fluctuations of the liquid. Experiments at higher gradients reveal a time-periodic flow regime with frequencies down to cycles per hour. These observations lend support to modern theories for the transition to turbulence.

1.34 Adsorbed layers of D_2, H_2, O_2, and ^3He on graphite studied by neutron scattering[§]

(M. Nielsen, J.P. McTague (University of California, California), and W. D. Ellenson (Brookhaven National Laboratory, New York, USA))

The phase diagrams (Fig. 18) of adsorbed monolayers of D_2, H_2, O_2, and ^3He on graphite were measured by neutron diffraction. H_2- and D_2-layers have a registered $\sqrt{3}$ structure at low coverages, and at monolayer completion they have a dense triangular structure, which is incommensurable with the substrate. Between the two densities there is a broad region of coverages where the structure is triangular but the lattice parameter varies with coverage. Adsorbed O_2-layers are found to have three distinct phases which are all incommensurable with the substrate lattice. Because of the large absorption cross section of ^3He, neutron diffraction measurements on the ^3He layers are much more difficult, but both the registered $\sqrt{3}$ structure and the dense triangular structure near monolayer completion were observed.

1.35 Experiments with H_2 on grafoil and alumina

(M. Nielsen, W.D. Ellenson (Brookhaven National Laboratory, New York, USA) and I. Silvera (Natuurkundig Laboratorium, Amsterdam, The Netherlands))

Monolayers of adsorbed H_2 and D_2 on grafoil were studied by

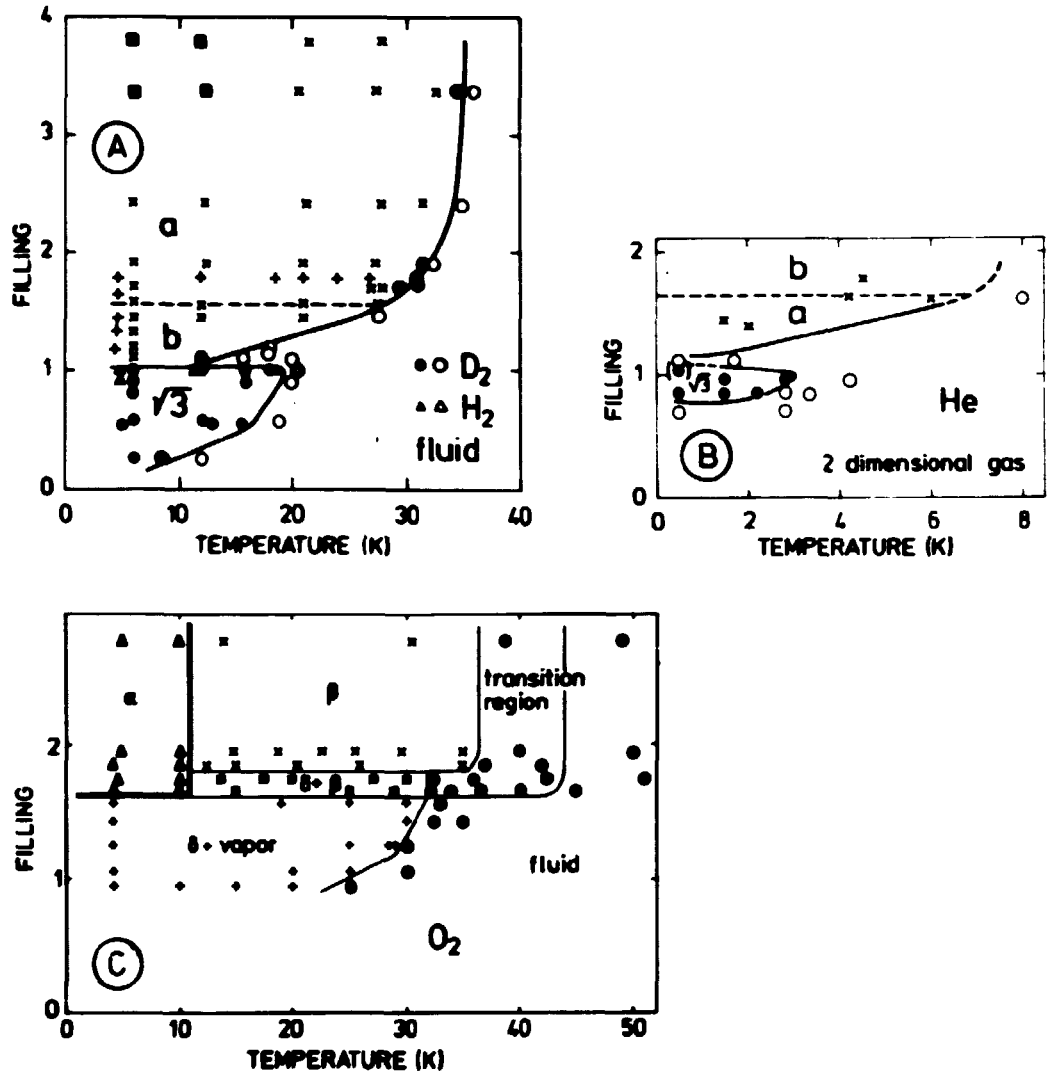

Fig. 18 Phase diagrams for D_2, H_2, ^4He, and O_2 layers adsorbed on grafoil. The filling is the amount of gas adsorbed, measured in units of the amount of gas needed to complete the commensurable, $\sqrt{3}$ structure. The points show where diffraction peaks were observed or looked for. (A) (●) D_2 and ▲ H_2 layers in the $\sqrt{3}$-phase, (×) D_2 and (+) H_2 layers in the b- and a-phase, (○) D_2 and (△) H_2 in the fluid phase ⊠ D_2 layers giving deformed groups with high background. The dashed line indicates the start of promotion to the second layer. (B) adsorbed ^4He layers. The dashed line indicates the start of promotion to the second layer. In phase b the first layer has an even lateral triangular structure with a_0 = 3.32 Å and in this region the triangular structure is expanding continuously with decreasing filling. (C) Adsorbed O_2 layers. The monolayer completion coincides with the α to (δ + vapor) phase boundary.

elastic and inelastic neutron scattering. At low coverages, a registered $\sqrt{3}$ phase was found and at high coverages a dense triangular structure, which is incommensurable with the substrate. Between these two phases there exists a broad region where the structure is triangular but the lattice parameter varies continuously with the coverage. The inelastic response from the H_2 and D_2 layers shows a localized oscillator behaviour in the $\sqrt{3}$-phase and a broad spectrum of frequencies in the dense regime. We have also studied the inelastic neutron scattering from H_2-layers adsorbed on activated alumina. In this case the molecular rotations were found to be partly quenched in contrast to the case for H_2-layers on grafoil. From the neutron scattering spectrum and measurements of the separation coefficients, it is concluded that the H_2 molecules adsorbed on alumina behave like axially constrained rotors.

1.36 Dynamics of SnI_4

(I.U. Heilmann)

The molecular crystal tin-tetraiodide, SnI_4, is an extremely compressible substance with a large thermal expansion, thus exhibiting bulk properties that indicate soft, anharmonic intermolecular interactions. Both the structure and the lattice dynamics of this material were studied by means of neutron elastic and inelastic scattering at various temperatures using single crystals prepared at Risø. After trying out a couple of techniques, the most effective way of producing larger crystals proved to be the Bridgeman method, and high quality single crystals up to approximately 10 cm^3 were obtained.

In contrast to the majority of molecular crystals having rather low symmetry, SnI_4 crystallizes in the cubic space group Pa3 with 8 molecules in the unit cell (a = 12.27 Å at 295 K). The structure was originally determined by Dickenson (1923) and later studied by Meller and Frankuchen (1955) and by Percy et al. (1975). All the earlier studies were by X-ray diffraction methods in contrast to the present structural study by neutron diffraction. The measurements were performed at 128 and 295 K and compared to several structural models. The results agree with the X-ray studies. In addition it was found that higher order cumulants play only a minor role, if any, in the atomic

structure factors. Furthermore, it may be concluded that the atomic temperature factors in SnI_4 are fairly well described in a model assuming isotropic translational and librational motion of rigid, regular tetrahedral molecules. Finally, it could be shown that the shape and size of the molecule are independent of temperature and that the large thermal expansion predominantly arises from the intermolecular potentials.

The phonon measurements were preceded by lattice dynamics calculations based on Pawley's (1972) formulation of the dynamical problem of molecular crystals. In this formulation it is assumed that the intramolecular forces are much stronger than the intermolecular forces and that the molecules can be considered as rigid. In the present case it was assumed that the rigid molecules interact through

$$V(r,K) = - A_k r^{-6} + B_k e^{-\alpha_k r},$$

where k indicates the particular chemical pairing (e.g., Sn-Sn, I-I, or Sn-I). These calculations allowed for a reliable assignment of the various phonon peaks observed by neutron scattering. Dispersion relations at room temperature were measured in the three high-symmetry directions and selected modes were also measured at 43, 82, 162, 343, and 393 K in order to determine shifts in the mode frequencies and in the line widths of the phonon groups. Figure 19 presents, as an example, the dispersion

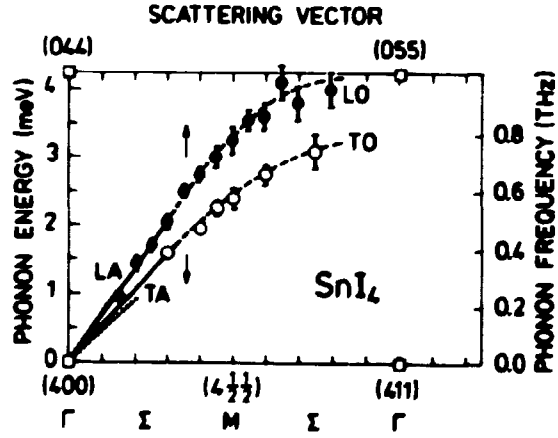

Fig.19 Observed room temperature phonon frequencies in SnI_4 for wavevectors $\vec{q} = (0,\xi,\xi)$. The scattering vector $\vec{\kappa}$ for filled and open circles is indicated above and below, respectively. The dotted lines result from the lattice dynamic calculations.

relations at room temperature in the [0ξξ] direction. The agreement between the calculated and the measured phonon energies was surprisingly good. The effect of anharmonicity could be easily seen from the temperature dependence of the frequency shifts and the increase of the widths of the phonon groups as the temperature is increased. The results obtained by neutron scattering are in agreement with the results obtained using Raman and Mössbauer spectroscopy (Heilman 1977).

1.37 Diffusion in the high temperature ionic conductor $SrCl_2$
(J.K. Kjems and M. Dickens (AERE, Harwell, U.K.))

$SrCl_2$ belongs to the class of ionic conductors often named the fluorites because of the common CaF_2 crystal structure. In $SrCl_2$ the ionic conductivity changes rapidly above 923 K and the specific heat shows a broad anomaly which peaks at 508 K, the whole anomaly being associated with an increasing mobility and consequent disorder among the Cl^- ions. Preliminary inelastic neutron scattering data on a single crystal of $SrCl_2$ have shown temperature-dependent quasi-elastic scattering whose intensity changes rapidly in the temperature range 973-1103 K. The scattering is most pronounced along the [100] direction and it is unobservable along the <011> directions. Experiments are in progress and it is planned to examine isotopically enriched samples in order to establish the relative contributions of coherent and incoherent scattering.

1.38 Quasi-elastic neutron scattering in para-azoxyanisole
(N. Niimura, H. Bjerrum Møller, and T. Riste (IFA, Kjeller, Norway))

The neutron scattering from normal protonated (p-PAA) and deuterated (d-PAA) para-azoxyanisole was measured in the isotropic liquid phase at momentum transfers $0.8\ Å^{-1} < Q < 5\ Å^{-1}$ and energy transfers up to 25 meV. For p-PAA, the spectra can be interpreted by means of a model of continuous, uniaxial rotational diffusion around the long molecular axis with diffusion coefficient D = 0.18 meV. For d-PAA, which is a coherent scatterer, the structure of the liquid manifests itself through the structure factor S(Q), which modulates the scattered intensity

and introduces an energy narrowing (de Gennes narrowing) at the maxima of S(Q). Data on unoriented samples of d-PAA in the nematic phase are indistinguishable from those derived from measurements in the isotropic phase, which suggests that there are no collective excitations of the nematic phase.

1.39 Universal X-ray spectrometer*

(J. Als-Nielsen and B. Buras)

A universal X-ray spectrometer intended for studies of the physics of condensed matter is under construction. It is especially designed for diffuse X-ray scattering, phase transformation studies and time-resolved studies. The spectrometer is transportable and suited for work both at the DORIS synchrotron storage ring in Hamburg and with a rotating anode, X-ray generator in Denmark. Two modes of operation are envisaged: the triple-axis mode and the energy-dispersive mode.

1.40 Optimum resolution in X-ray energy-dispersive diffractometry

(B. Buras, N. Niimura, and J. Staun Olsen (University of Copenhagen))

The resolution problem in X-ray energy-dispersive diffractometry was discussed in some detail and the dependence of the full width at half maximum (δd_{FWHM}) was calculated as a function of the interplanar spacing and the scattering angle for different divergences ($\Delta\theta_o$) of the incident X-ray beam and different characteristics of the solid state detector system. Figure 20 presents typical results for an average quality extra-pure Ge-detector system. The most striking feature is the existence of a pronounced minimum at small scattering angles for the small divergences $\Delta\theta_o$ characteristic of X-ray synchrotron radiation. However, small scattering angles require large photon energies. Thus, for measurements with high resolution, synchrotron storage rings should emit an X-ray spectrum extending far into the high-energy photon region (up to 100 keV and higher) if energy-dispersive diffractometry is to be used. The formula derived for δd_{FWHM}

---

* Joint project of the Physics Department, Risø National Laboratory, and the Physics Laboratory II, University of Copenhagen, supported by the Danish Natural Science Research Council.

enables calculation of the optimum scattering angle for a given characteristic of the solid state detector system and a given range of interplanar spacings for any given divergence of the incident and scattered beams.

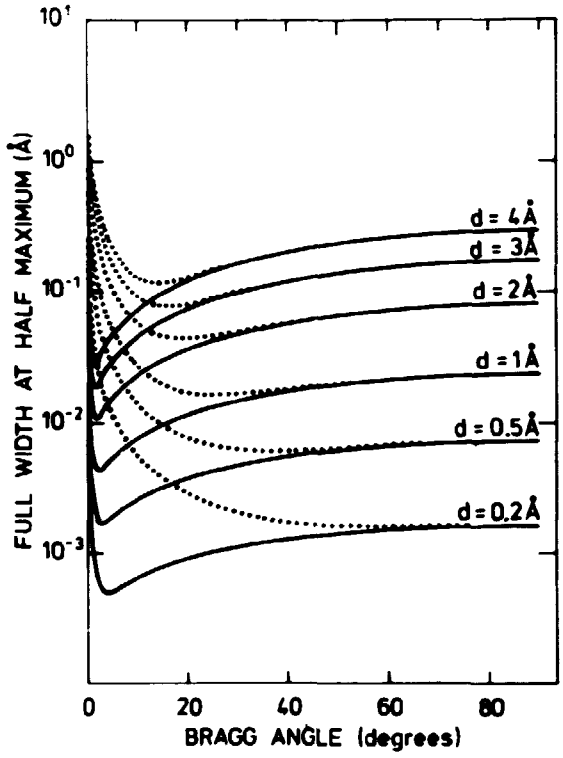

Fig. 20 Calculated dependence of the full width at half maximum of the Bragg angle for different interplanar spacings in energy-dispersive diffractometry. The full and dotted lines are calculated for $\Delta\theta_o = 10^{-4}$ rad and $\Delta\theta_o = 5 \cdot 10^{-3}$ rad, respectively.

1.41 References (see also 5.2)

BAK, P., KRINSKY, S. and MUKAMEL, D. (1976). Phys. Rev. Lett. 36, 52-55.

BRAUER, G. and ZAPP, K.H. (1954). Z. Anorg. Allg. Chem. 102, 1311-1316.

BURAS, B., KOFOED, W., LEBECH, B., and BÄCKSTRÖM, G. (1977). Risø Report No. 357.

DICKENSON, R.G. (1923). J. Amer. Chem. Soc. 45, 958-962.

GROVER, B. (1965). Phys. Rev. A140, 1944-1951.

GUERTIN, R.P. (1977). In: Electron-Phonon Interaction and Phase Transitions. Edited by T. Riste (Plenum Press) New York, 248-257.

HAZELL, A.C., LARSEN, F.K., and LEHMAN, M.S. (1972). Acta Cryst. B28, 2977-2984.

HEILMANN, I.U. (1977). Ph. D. Thesis, University of Copenhagen, Denmark (and references therein).

LEBECH, B. and RAINFORD, B.D. (1974). Proc. Int. Conf. Magn. Moscow 1973, 3, 191-195.

LINDGÅRD, P.-A. (1978a). Excitations and spin waves. To be published in the proceedings of the Conference on Rare Earth Metals and Actinides, Durham, U.K., July 4-8, 1977.

LINDGÅRD, P.-A. (1978b). Phase transitions and critical phenomena. In: Topics in Current Physics. "Neutron scattering" Edited by H. Dachs (Springer Verlag) Berlin. Chapter 6, 197-241. (To be published).

LINDGÅRD, P.-A. and KOWALSKA, A. (1976). J. Phys. C: Solid State Phys. 9, 2081-2092.

MACKENZIE, G.A., ARTHUR, J.W., and PAWLEY, G.S. (1977). J. Phys. C: Solid State Phys. 10, 1133-1149.

MACKINTOSH, A.R. (1977). Physics Today 30, 23-30.

McMILLAN, W.L. (1975). Phys. Rev. B14, 1496-1502.

MELLER, F., and FANKUCHEN, I. (1955). Acta Cryst. 8, 343-344.

MERMIN, N.D. and WAGNER, H. (1966). Phys. Rev. Lett. 17, 1133-1136.

MOON, R.M., CABLE, J.W., and KOEHLER, W.C. (1964). J. Appl. Phys. 33, 1041-1042.

MUKAMEL, D. and KRINSKY, S. (1976). Phys. Rev. B13, 5065-5077, 5078-5085.

NIELSEN, O.V., LEBECH, B., LARSEN, F.K., HOLMES, L.M., and BALLMAN, A.A. (1976). J. Phys. C: Solid State Phys. 9, 2401-2411.

PAWLEY, G.S. (1972). Phys. stat. sol. (b) 49, 475-488.

PAWLEY, G.S. and DIETRICH, O.W. (1975). J. Phys. C: Solid State Phys. 8, 2549-2558.

PAWLEY, G.S., MACKENZIE, G.A., and DIETRICH, O.W. (1977). Acta Cryst. A33, 142-145.

PEERCY, P.S., SAMARA, G.A , and MOROSIN, B. (1975). J. Phys. Chem. Solids, 36, 1123-1128.

SMITH, H.G. and GLÄSER (1970). Phys. Rev. Lett. 25, 1611-1613.

STEPHENSON, J. (1970). Phys. Rev. B1, 4405-4409.

TRAMMEL, G.T. (1960). J. Appl. Phys. 31, 3625-3635.

WEBER, W. (1973). Phys. Rev. B8, 5082-5092, 5093-5097.
ZALLEN, R., GRIFFITHS, C.H., SLADE, M.L., HAYEK, M., and BROFMAN, O. (1976). Chem. Phys. Lett. 39 (1), 85-89.

2. PLASMA PHYSICS

The plasma physics section works under a contract of association between the Risø National Laboratory and Euratom. The activities are centered on technology of interest for future fusion reactors (2.1-2.10, 2.25-2.26) and on basic plasma physics (2.11-2.24). The technological aspects of plasma physics are studied with one of the possible refuelling schemes for fusion reactors in mind. This scheme requires an acceleration technique able to accelerate small pellets to a velocity of the order of 10^3-10^4 m/s. The velocity necessary depends on the ablation rate of a pellet inside a fusion plasma. Studies of interactions between plasmas and solids are therefore of interest. Two basically different approaches are adopted. One (2.1-2.7) is a study of the interactions of a controlled beam of charged particles with films of solid hydrogens. The other (2.8-2.10) is an investigation of the interactions between a Tokamak plasma and solid pellets of solid hydrogens. A small Tokamak, "Dante", was constructed for this study.

The main object of basic research in plasma physics is to investigate waves and instabilities in a relatively cold steady state plasma (produced in a Q-machine). Turbulence, ion-cyclotron waves, and ion-acoustic waves in the presence of electron plasma waves are the chief phenomena investigated.

2.1 Penetration depth of 0.5-3 keV electrons in solid H_2 and D_2

(J. Schou and H. Sørensen)

The mirror substrate method was used for measuring the penetration depth of 0.5-3 keV electrons in solid H_2 and D_2. The penetration depth was found to be $0.53 \cdot 10^{18} \times E^{1.72}$ molecules/cm^2 with the energy given in keV. There was satisfactory agreement with other data. The measurements also showed that the escape depth for true secondary electrons from solid D_2 is below 50 Å, which agrees well with the small values for the secondary electron emission coefficient found for solid D_2. Results were furthermore obtained for the electron reflection coefficient, i.e. the number of electrons that are reflected with high energies for the Au-substrate. The electron reflection coefficient

agrees well with other results both with respect to magnitude and to energy dependence.

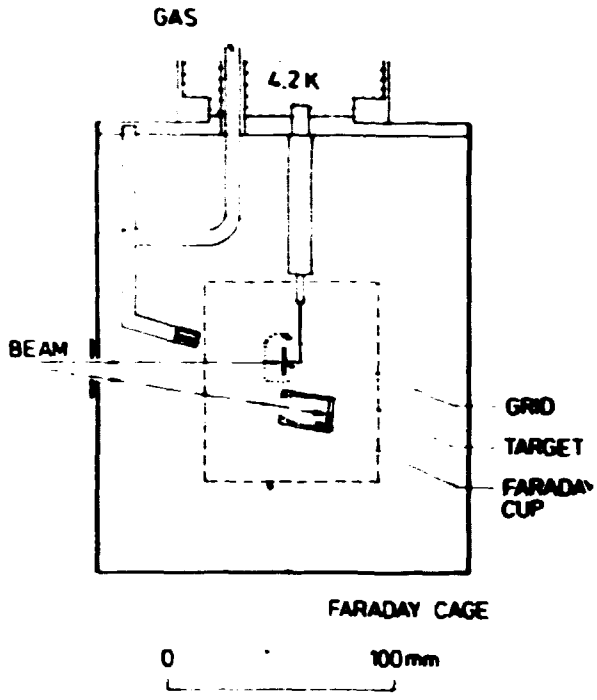

Fig. 21 A schematic drawing of the target region in the set-up used for studies of secondary electron emission. The target region is situated below the liquid He-cryostat.

2.2 Interaction between solid N_2 and 1-3 keV electrons

(H. Sørensen and J. Schou)

An improved experimental set-up was built in a new cryostat for studies of secondary electron emission. The set-up includes a Faraday-cup placed below the target, as shown in Fig. 21. This means that the beam current can be measured independently of the state of the target surface. It is then possible to measure both the secondary electron emission coefficient and the electron reflection coefficient for incidence of electrons. The new set-up was first used for studies of the normal incidence of electrons on solid N_2. It is also used for studies of the oblique incidence of electrons on solid H_2 and D_2.

Experimental studies were made of the interaction between solid N_2 and beams of 1-3 keV electrons. The projected range for the electrons was measured by means of the mirror substrate method (Au-substrate), giving the result $9.02 \cdot 10^{16} \cdot E^{1.75}$ molecules/cm^2 with the energy given in keV (Fig. 22). The escape

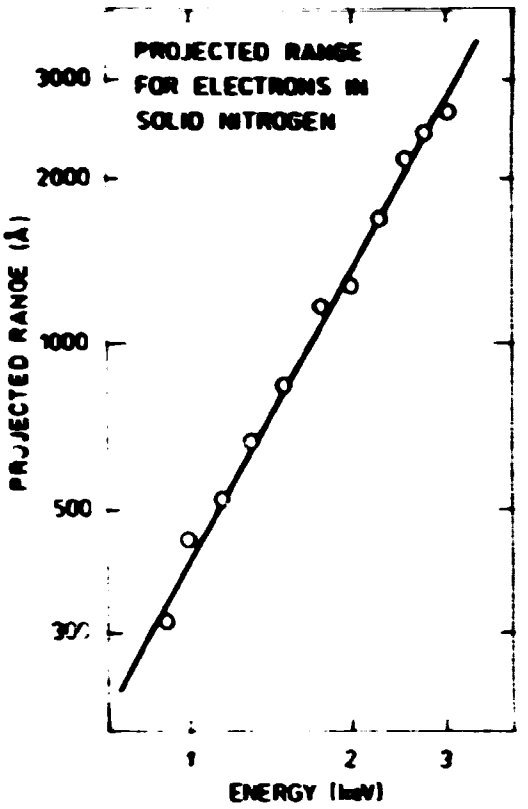

Fig. 22 The projected range for 1-3 keV electrons in solid N_2. 1 Å corresponds to $2.21 \cdot 10^{16}$ molecules/cm^2.

depth for secondary electrons was studied by means of the equivalent substrate method (C-substrate). The results varied from 280 Å at 1 keV to 400 Å at 3 keV. Measurements were also made of the secondary electron emission coefficient, which varied from 2.3 el/el at 1 keV to 1.2 el/el at 3 keV, and of the electron reflection coefficient, which varied from 0.17 at 1 keV to 0.13 at 3 keV. Moreover, measurements were made of the electron reflection coefficient for the C-substrate; the results varied from 0.13 at 1 keV to 0.12 at 3 keV. The agreement of these observations with other theoretical and experimental results ranges from good to fair.

2.3 On secondary electron emission from solid H_2 and D_2

(H. Sørensen and J. Schou)

Improvement of the set-up used for studies of secondary electron emission enabled us to make measurements of secondary electron emission from solid hydrogens also at oblique incidence of electrons (Fig. 21). Studies of secondary electron emission

(SEE) from solid H_2 and D_2 were therefore made for the incidence of electrons up to 3 keV and for the incidence of hydrogen, deuterium, and helium ions up to 10 keV, both for normal and oblique incidence. The SEE coefficient for solid H_2 is always around 0.65-0.70 times that for solid D_2. This difference is attributed to different losses to vibrational molecular states in H_2 and D_2 for the low-energy electrons (Sørensen 1977). Measurements were also made on solid para-H_2 with both electrons and H-ions (Fig. 23). The results did not differ from those for normal H_2.

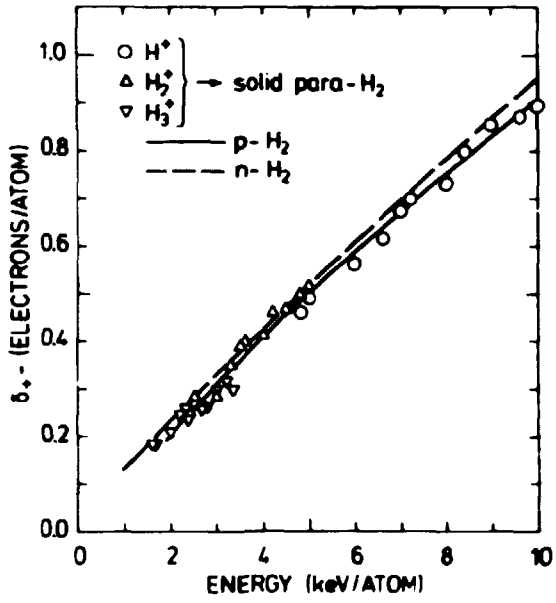

Fig. 23 The secondary electron emission coefficient for incidence of hydrogen ions on solid para-H_2. The solid curve is a parabolic fit to the data, while the dashed curve is a parabolic fit to the data for incidence on normal H_2.

For normal incidence of hydrogen and deuterium ions on D_2, the SEE coefficient may be written $\delta = -2.786 + 2.857(1 + 0.1073E)^{\frac{1}{2}}$ el/atom for 10 keV $\geq E \geq$ 0.6 keV, where the energy is the particle energy in keV/a.m.u. For oblique incidence, the coefficient increases with increasing angle of incidence θ, and at the largest energies it is found that $\delta(\theta) = \delta(0)/\cos\theta$, up to 75°. The number of positive, low energy secondary ions is small at normal incidence, and it is seen that it increases strongly with increasing angle of incidence.

For normal incidence of helium ions on D_2, the SEE coefficient may be given by $\delta = (0.414 + 0.0311E)$ el/ion for 10 keV $\geq E \geq$

4 keV, where E is the particle energy. For normal incidence of electrons on D_2, the SEE coefficient may be written $\delta = (0.197 + 0.0736E - 0.0118E^2)/E$ el/el for 3 keV $\geq E \geq$ 0.5 keV. For oblique incidence of electrons, the variation with the angle is stronger than for the incidence of ions, and for smaller angles it is roughly $\delta(\theta) = \delta(0)/(\cos\theta)^{3/2}$. For normal incidence the number of reflected electrons is insignificant; it increases strongly with the angle of incidence to around 0.1 el/el at 60° for both H_2 and D_2.

2.4 Energy reflections from Nb, Ag, and Au bombarded by 1-10 keV protons[§]

(H. Sørensen)

The calorimetric D_2-film method (Sørensen 1976), which operates at 4.2 K, was used for measuring the energy reflection coefficient γ at normal incidence of 1-10 keV protons on Nb, Ag, and Au. H_2^+ and H_3^+ ions were used to obtain the lowest velocities. The data are given as a function of the reduced energy ε, and the results for Nb are lower than those for Ag and Au. Data for Ag and Au agree with data published by Andersen et al. (1976) and by Sidenius et al. (1976), in agreement with the rule that, for several materials, γ only depends on the material through the reduced energy ε. Some metals such as Nb deviate from this rule; the data for Nb are below the universal curve, similar to the data for Sidenius et al. for Nb, Mo, and Ta. The origin of this deviation is unknown. A comparison was made with the theoretical results of Robinson (1974), Vucanić and Sigmund (1976a), Littmark and Maderlechner (1976), and Oen and Robinson (1976a); the agreement being in general good.

2.5 Energy reflection coefficients for 5-10 keV helium-ions incident on Au, Ag, and Cu

(J. Schou, H. Sørensen, and U. Littmark (H.C. Ørsted Institute, University of Copenhagen))

The calorimetric D_2-film method was also used for measurement of the energy reflection coefficient γ for normal incidence of 5-10 keV helium-ions on Au, Ag, and Cu. A theoretical calculation of γ by means of transport theory (Littmark and Maderlechner 1976) gives somewhat higher values.

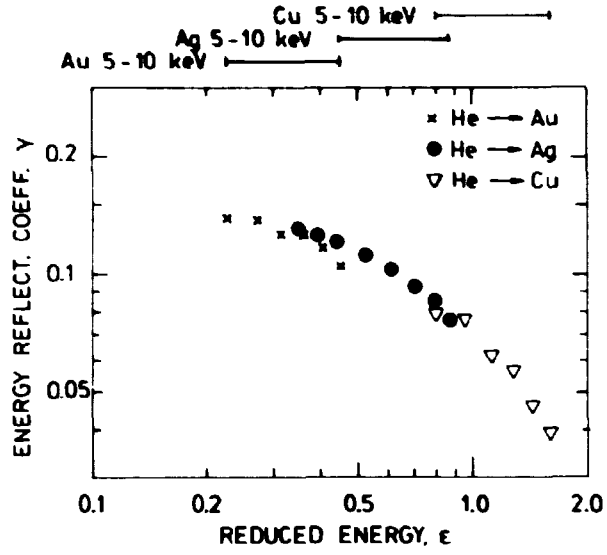

Fig. 24 The energy reflection coefficient for normal incidence of helium-ions on Au, Ag, and Cu as a function of the reduced energy.

The experimental data are given as a function of the reduced energy ε and they agree well with the rule that, for several materials, γ only depends on the material through the reduced energy (Fig. 24). There is fair agreement with other experimental data of Andersen et al. (1976) and of Hildebrandt and Manns (1976). A comparison was made with the theoretical results of Robinson et al. (1976), of Oen and Robinson (1976b), and of Vucanić and Sigmund (1976b).

It is observed that within the energy range covered here, i.e. $0.2 < \varepsilon < 2$, the measured energy reflection coefficient for He ions is around 20% higher than that for hydrogen ions with the same values of ε.

2.6 Secondary electron emission from electron and ion incidence on solids

(J. Schou and P. Sigmund (H.C. Ørsted Institute, University of Copenhagen))

A theoretical treatment was made of secondary electron emission from a random infinite solid caused by the incidence of electrons or ions. The energy spectrum and the angular distribution of the secondary electron yield are obtained as a solution of the Boltzmann transport equation.

During the slowing-down of the incoming beam particle, a fraction of the energy of the incoming particle is deposited in electronic excitation and ionization. Following the principles of sputtering theory (Sigmund 1969), the yield is proportional to the surface value of the distribution of the deposited energy. The yield is compared with recent measurements by Holmén et al. (1977) for light and heavy ions. For heavy ions, the influence of recoiling target atoms was estimated.

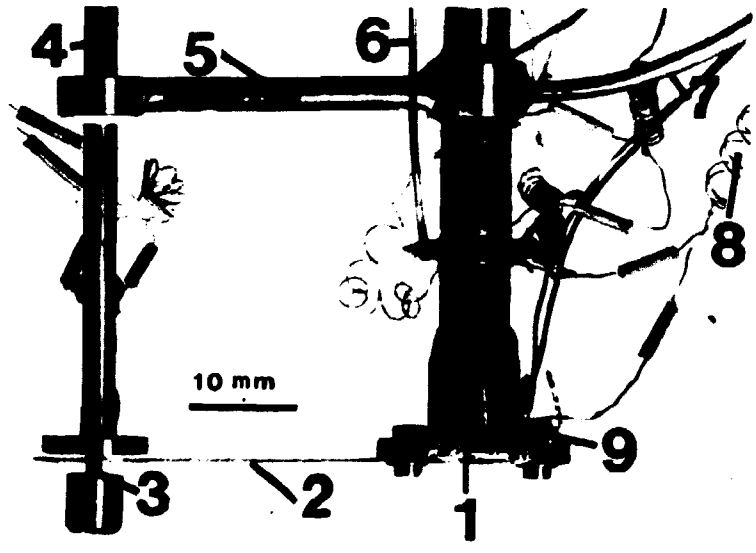

Fig. 25 Photograph showing details of the set-up used for the extrusion of solid H_2 and D_2 filament (see 2.7). (1) Chamber with a heater winding. (2) Knife. (3) Eccentric used for moving the knife. (4) Rotating shaft. (5) Mechanical support. (6) Copper wire for thermal connection. (7) Gas tube. (8) Electrical wire. (9) Carbon resistance thermometer. A enlarged photograph of the lower part of the chamber is shown in Fig. 26.

2.7 Extrusion of solid H_2 and D_2

(A. Nordskov, J. Schou, H. Skovgård, and H. Sørensen)

For studies of pellet-plasma interaction it is mandatory to have pellets of solid H_2 or D_2, and a set-up was thus built in which filaments of these solids can be extruded. Gas is led into a chamber placed below the bottom of a liquid He-cryostat. Here, the gas solidifies and when the chamber is full, the solidified gas is compressed with a piston to form a dense mass. The chamber is then heated to a temperature of $\sim$ 10-13 K with an electrical heater, and the solid H_2 or D_2 can be extruded

through a nozzle at the bottom of the chamber. Filaments of solid H_2 and D_2, 1 mm in diameter, were made in this manner. The set-up is placed behind radiation shields affording protection against thermal radiation, and the extrusion chamber can only be observed through a 2 cm hole in the shields. Under these circumstances, i.e. protected against thermal radiation, a filament does not change visibly when kept for one hour. The temperature at which the extrusion is made differs for H_2 and D_2. The pressures at which the extrusion is made are also different; a pressure of 60 bar is applied to the solid D_2 while a somewhat lower pressure is applied to the solid H_2.

An attempt was made to cut a D_2 filament with a knife made of phosphor-bronze, the knife being moved by means of an eccentric placed on the end of a revolting shaft. However, the piece of filament cut off adhered to the knife. Apparently solid D_2 is sticky. Figure 25 is a photograph of the chamber, and Fig. 26 is a photograph of the bottom of the chamber with a filament of solid D_2 protruding.

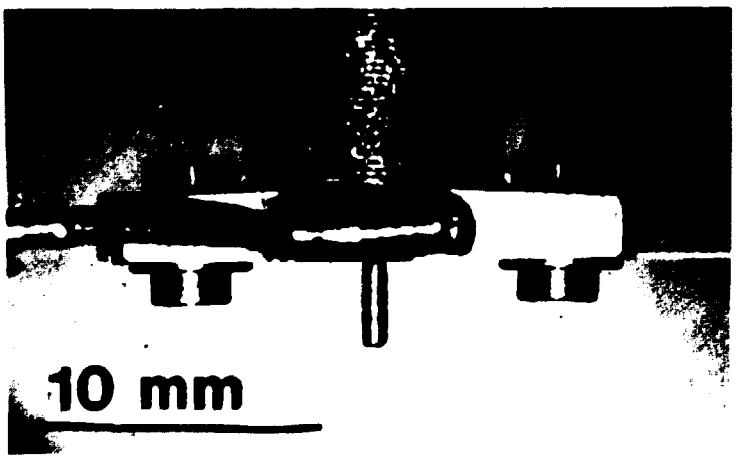

Fig. 26 An enlargement of the lower part of the chamber in the set-up used for the extrusion of H_2 or D_2 filaments (see 2.7).

2.8 Hydrogen pellet-rotating plasma interaction: A spectroscopic analysis

(L.W. Jørgensen, A.H. Sillesen, and P. Øster)

Spectroscopic measurements were made on the interaction between solid H_2 pellets and rotating plasmas. It was found that the light emitted is specific to the pellet material, and that the

velocity of the ablated H-atoms is of the order of 10^4 m/s. The investigation was carried out with a view to the possible refuelling of fusion reactors by the injection of pellets.

2.9 Pellet refuelling programme

(V. Andersen, L.W. Jørgensen, C.T. Chang, P. Nielsen, and A.H. Sillesen)

Pellet refuelling studies were carried out using the Puffatron device. The ablation rates found in these studies were reported by Jørgensen et al. (1975). More recent measurements give details of the interaction mechanism between pellet and plasma (see 2.8), and these measurements seem to agree well with the prevailing theory. In this theory the ablated neutrals form a gas shield around the pellet, and a balance is set up between the incident energy-flux and the gas density in the shielding cloud. In the new Tokamak experiment DANTE described in 2.25, particular emphasis will be laid on a proposed method for simulating high pellet injection velocities by moving the plasma column in the vertical direction, rather than developing more elaborate pellet guns.

2.10 Determination of the ion velocity distribution in a rotating plasma from measurements of Doppler broadening

(L.W. Jørgensen and A.H. Sillesen)

The Doppler-broadened profile of He II 4685, 75 Å was measured along a chord in a rotating plasma, transverse to the magnetic field. Using a single-orbit picture, the corresponding velocity spectrum of ions was calculated. These results confirm the measurements, so it can be concluded that the single-orbit picture is valid for the discharge period under investigation, except for the first few μs during breakdown when a strong interaction between the plasma and the remaining neutral gas takes place by Alfvén's critical velocity mechanism. A simple relation is given between the measured half-width and shift of the Doppler profile and the macroscopic quantities of ion velocity and energy. Several Doppler-broadened profiles are shown for different plasma parameters.

2.11 On the use of Langmuir probes in a laser-produced plasma§

(C.T. Chang*)

In a plasma produced by irradiating a solid target with a laser beam, it was found that Langmuir probes can be used to determine both the electron temperature T_e and the number density n_e in the asymptotic expansion phase - in addition to their use for time-of-flight measurements. In the immediate vicinity of the target, the successful application of the probe is doubtful. Although the determination of T_e might be difficult in the intermediate region, the electron number density n_e can still be determined from the ion saturation current. Based on a repeated guess of the plasma potential, an iterative method was found for the determination of T_e to a better accuracy in the asymptotic expansion phase.

2.12 Study of a laser-produced plasma by Langmuir probes§

(C.T. Chang*, M. Hashmi+, and H.C. Pant+ (+Max Planck Institute of Plasma Physics, Garching, F.R.G.))

The structure, the parameters and the expansion or the plasma produced by focusing a 7 J, 20 ns Nd glass laser on stainless-steel and glass targets suspended in a high-vacuum chamber were investigated by means of Langmuir probes. It was observed that the probe signals consisted of a photo-electric emission peak and the main plasma from the target. The flow velocity, density and electron temperature of the plasma were determined. The expansion of the plasma was found to be adiabatic, yielding $\gamma = 5/3$. The spatial distribution of the plasma was observed to be strongly anisotropic.

2.13 Oscillation modes of a laser-produced plasma expanding into a uniform magnetic field§

C.T. Chang* and M. Hashmi (Max Planck Institute of Plasma Physics, Garching, F.R.G.))

The oscillation made of a laser-produced plasma expanding into a uniform transverse magnetic field, B_o, is seen to depend on the

---

* Work performed at the Max-Planck Institute of Plasma Physics, Garching, F.R.G.

similarity parameter $N = (8\pi\rho_o)^{\frac{1}{2}} v_o/B_o$, where ρ_o, v_o are the mass density and velocity of the expanding plasma, respectively. Experimental results revealed the existence of a transition phenomena, namely, that there exists a critical value, N^*, for $N > N^*$, where the oscillations of the ion current as detected by a probe are regular. For $N < N^*$, random oscillations appear.

2.14 Nonlinear Langmuir wave modulation in collisionless plasmas

(K.B. Dysthe (University of Tromsö, Norway) and H.L. Pécseli)

A nonlinear Schrödinger equation for Langmuir waves was derived by using a fluid model for the electrons, while both a fluid and a Vlasov formulation were considered for the ion dynamics. It was found that the two formulations lead to significant differences in the final results, especially in the expressions concerning the modulational instability of a plane Langmuir wave. It was thus demonstrated that when the Vlasov equation for the ions is applied, a Langmuir wave is modulationally unstable for arbitrary perturbations independent of the unperturbed wave amplitude, in contrast to what is found for fluid ions. A simple analogy with negative energy waves explaining the different features of the two cases was outlined. The theory was extended to cover the case where a weak magnetic field is important for the ion dynamics. In this case the amplitude-modulated Langmuir wave train may resonate with electrostatic ion cyclotron waves in addition to with ion acoustic waves. The presence of the former resonance introduces profound changes in the modulational stability of the Langmuir wave.

2.15 Nonlinear propagation of electron plasma waves in magnetized plasmas

(K.B. Dysthe*, E. Mjølhus* (* University of Tromsø, Norway), H.L. Pécseli, and L. Stenflo (University of Umeå, Sweden))

Propagation of nonlinear high-frequency plasma waves in magnetized plasma was considered. The analysis was restricted to cases where the electron plasma frequency is considerably larger than the electron cyclotron frequency. The modulational stability of the waves was investigated paying particular attention to the influence of thermal effects arising from a spatially varying electron temperature induced by the spatially varying electron

heating in the amplitude modulated wave train. The possibility of solitary modulations was also considered.

2.16 Numerical simulation of nonlinear electron plasma oscillations

(V. Turikov)

A computer program for numerical simulation of nonlinear oscillations in the Q-machine plasma column was developed. The particle-in-cell method with area-weighted electron charge was used in this program. Electric field values were calculated by quadratic interpolation of the potential values at the three nearest nodes of the space mesh. The influence of finite plasma radial dimension was taken into account by use of the extra linear term in the Poisson equation describing the zero-order Trivelpiece-Gould mode. Preliminary results show that the simulation model used has quite high accuracy and also that there is good agreement with the two-stream instability simulation results. The program will be used for numerical investigation of the nonlinear response of the Q-machine plasma to an external electric field impulse.

2.17 Finite-amplitude electron plasma waves in a cylindrical waveguide

(J. Juul Rasmussen)

The nonlinear behaviour of the electron plasma wave propagating in a cylindrical plasma waveguide immersed in an infinite axial magnetic field was investigated using the Krylov-Bogoliubov-Mitropolsky perturbation method. This method deduces the nonlinear Schrödinger equation governing the long-time slow modulation of the wave amplitude. From this equation the amplitude-dependent frequency and wavenumber shifts were calculated, and it was found that the electron waves with short wavelengths are modulationally unstable with respect to long-wavelength, low-frequency perturbations. It was further shown that an oscillatory solution of the Korteweg-de Vries equation, which is derived in the small wavenumber region, satisfies the small wavenumber limit of the nonlinear Schrödinger equation.

2.18 Formation and interaction of electron solitary holes in a collisionless plasma

(K. Saeki, P. Michelsen, H.L. Pécseli, and J. Juul Rasmussen)

An electron solitary hole is observed to propagate steadily in a collisionless magnetized plasma. In contrast to the soliton, the solitary hole does not damp even though its velocity is very near the electron thermal velocity. Two solitary holes attract each other and eventually coalesce. A computer simulation based on a water-bag model shows the particle motion in phase space, the excitation, and the propagation of the solitary hole.

2.19 Stationary density variation produced by a standing plasma wave

(P. Michelsen, H.L. Pécseli, J. Juul Rasmussen, and N. Sato (Tohoku University, Japan))

Measurements were made of a stationary density modulation produced by a standing electron plasma wave. The experimental results are well explained by taking into account the ponderomotive forces on the electrons exerted by the high frequency field. The results may be viewed as analogous to those obtained in an ordinary Kundt tube, that is often used to demonstrate standing acoustic waves.

2.20 Wave propagation in an ion-beam plasma system

(T.D. Jensen, P. Michelsen, and J. Juul Rasmussen)

The spatial evolution of a velocity or density-modulated ion beam is calculated for a stable and unstable ion beam plasma system, using the linearized Vlasov-Poisson equations. The propagation properties are found to be strongly dependent on the modulation form. In the case of velocity modulation, the perturbation initially grows and then shows a periodic change of amplitude along the beam, while in the case of density modulation only an instability causes growth. The results are in perfect agreement with experimental results published by Sato et al. (1977).

2.21 Energy transfer between potential energy and ions in ion acoustic waves

(J.P. Hansen and V.O. Jensen)

The problem of energy transfer between an ion acoustic wave in a collisionless plasma and the plasma ions is considered. The wave is described by the ion Vlasov-equation and the electron fluid-equation. In the limit of Quasi-neutrality, the equations reduce to

$$\frac{\partial f(x,v,t)}{\partial t} + v \frac{\partial f(x,v,t)}{\partial x} = \frac{c_e^2}{n_o} \frac{\partial n(x,t)}{\partial x} f_o'(v) \qquad (1)$$

and $n(x,t) = \int f(x,v,t)\, dv,$ (2)

where $n_o = \int f_o(v)dv$ and $c_e^2 = \kappa T_e/m_i$.

The wave is assumed to be excited at $x = 0$ with a perturbed distribution function

$$f(x = 0,v,t) = g(v)e^{iwt}. \qquad (3)$$

For cases where $f_o(v)$ and $g(v)$ are drifting Maxwellians, as in grid-excited waves in single-ended Q-machines, Eqs. (1) and (2) were solved with the boundary conditions (3) by Christoffersen et al. (1974) and Jensen and Michelsen (1972). It was found in general that a wave is damped with damping characteristics depending upon $g(v)$ and $f_o(v)$ and T_e.

The energy transfer between the potential energy of the damped wave and ions in the plasma is examined. In general, it is found that, averaged over one oscillating period, particles in $f_o(v)$ with <u>all</u> velocities absorb energy from the wave. The absorption spectrum in velocity space is peaked around the phase velocity of the wave but it is rather broad compared to $f_o(v)$. Ions initially in the perturbed distribution function $g(v)$ at $x = 0$ exchange energy with waves in a complicated manner depending upon velocity. Preliminary results were reported by Jensen (1976).

2.22. Temperature effect on the ion-beam-driven electrostatic ion cyclotron instability

(P. Michelsen, H.L. Pécseli, and J. Juul Rasmussen)

The electrostatic ion cyclotron instability (eici) is one of the microscopic instabilities that can be excited when an ion beam along a magnetic field traverses a plasma. The eici excited by drifting electrons was investigated several years ago (Motley and D'Angelo 1963, and Levine and Kuckes 1966), but it was found that the critical electron drift velocity increased with increasing electron temperature in contradiction to theoretical predictions.

Experimental investigations of the ion-beam-excited electrostatic ion cyclotron instability were performed in the Risø single-ended Q-machine, equipped with a microwave resonator that could raise the electron temperature by a factor of $\sim$ 10. A Na-ion beam was produced by means of an ion emitter, the bias of which determined the beam velocity. The ion distribution function was monitored by an electrostatic energy analyser.

When the ion beam exceeded a certain energy, oscillations near the ion cyclotron frequency were detected by an axially movable probe connected to a spectrum analyser. The dispersion relation of these waves confirmed that it was eici resulting from the interaction of a beam acoustic mode and an ion cyclotron mode. When the electron temperature was increased, the frequency of the unstable mode increased in agreement with the general electrostatic dispersion relation. Finally, the critical beam energy was found to decrease with increasing electron temperature, as expected from theory.

2.23 Interaction between ion acoustic waves and electron plasma waves

(P. Michelsen, H.L. Pécseli, and J. Juul Rasmussen)

The interaction between long-wavelength ion acoustic waves and short-wavelength electron plasma waves was examined in a low density Q-machine plasma. When the two waves were excited simultaneously, the electron wave became amplitude modulated, giving rise to ponderomotive forces acting on the electrons, and thus

in turn affecting the propagation characteristics of the ion acoustic waves. The influence of the electron plasma waves was to reduce the phase velocity and the damping distance of the ion acoustic wave. The experimental results are supported by theoretical considerations based on a simple model by introducing an effective electron temperature.

2.24 Ion-acoustic instability in the presence of high frequency oscillations

(J. Juul Rasmussen*, D. Sandu (Al.I.Cuza University, Rumania), and R. Schrittwieser (University of Innsbruck, Austria))

Measurements were made of a standing ion-acoustic wave instability, which was excited by a positively biased grid inserted perpendicularly into the plasma column of a single-ended Q-machine, under the influence of a high frequency signal superimposed onto the positive voltage at the grid. The experimental results show that in certain regions of the frequency and amplitude of the HF-signal the ion wave instability is stabilized or destabilized.

2.25 Current driven ion acoustic instability in a collisionless plasma

(P. Michelsen, H.L. Pécseli, J. Juul Rasmussen, and R. Schrittwieser (University of Innsbruck, Austria))

The current driven ion acoustic instability was investigated by means of an experiment performed in a collisionless plasma produced in a single ended Q-machine. Reflections at the ends of the plasma column gave rise to a standing wave. Parameters of the instability such as frequency versus wavelength and growth rate were investigated. Furthermore it was demonstrated that the fluctuations in the plasma column behaved as a classical Van der Pol oscillator. Accurate measurements of the growth rate of the instability could be performed by making explicit use of the particular properties of such a system.

---

*Work performed at the Institute of theoretical Physics, University of Insbruck, Austria.

[illegible]

[illegible] Nielsen

[illegible] Andersen et al. 1977) is now nearly [illegible] and has been operated for some months at reduced parameters compared to the design parameters. The toroidal field strength is [illegible].4 T and the plasma current [illegible] kA. The electrolytic capacitor-bank is not installed yet and the pulse duration is thus limited to [illegible] ms. The present phase of operation is useful in deciding how to obtain a good build-up of current

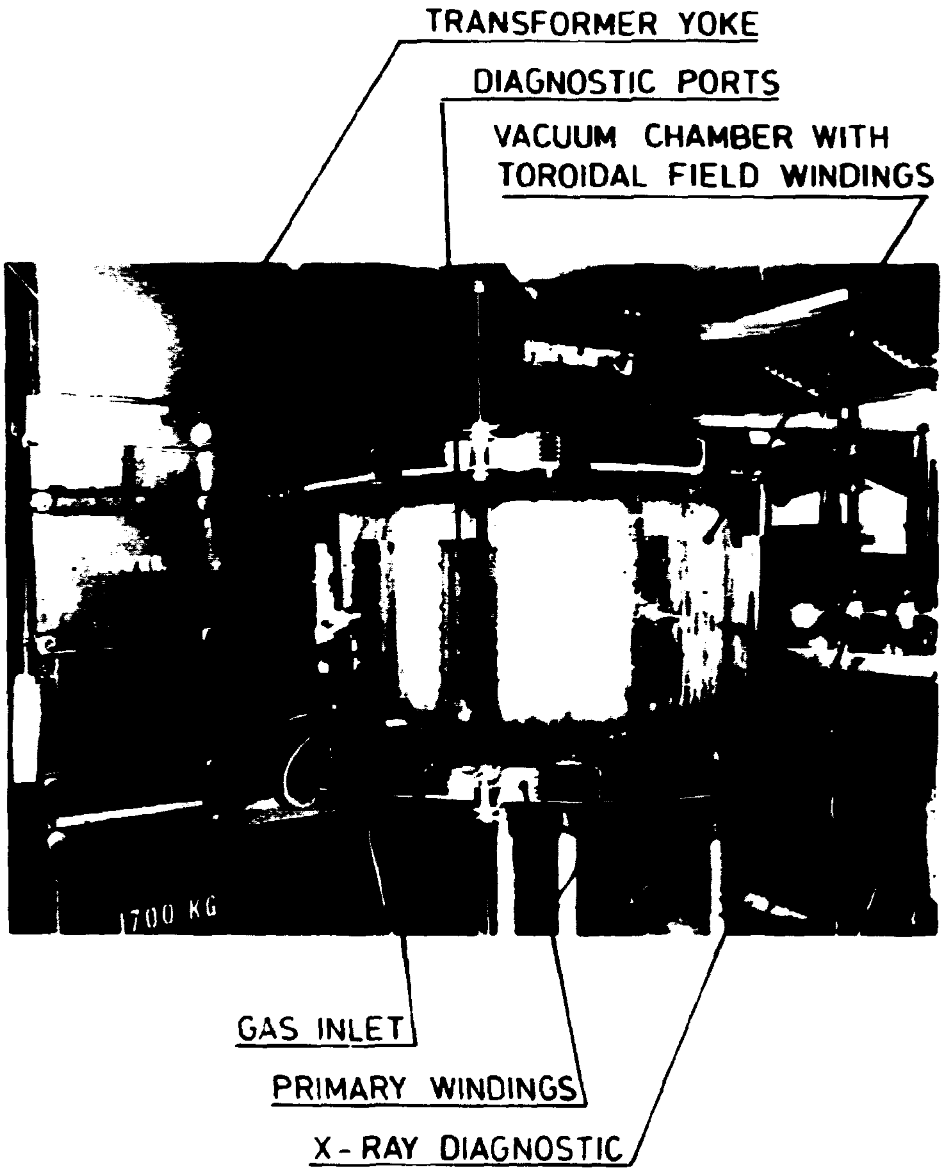

Fig. 27 The Danish Tokamak "Dante".

without disruptions, and also in developing the diagnostics and the interface of these with the computer system. Data taking and computer-processing are now routine operations. The principal diagnostics presently used are loops to measure induced voltage and current with local measurement of the toroidal field at the periphery of the plasma. The X-ray equipment is also ready and a new technique for data-processing developed. However, it appears that the present moderate temperature plasma has too low a temperature for X-ray detection.

The laser systems for measuring density and temperature are still under construction. Installation of the electrolytic capacitor-bank is almost complete. The upgrading to 0.8 T has been post-poned to the spring of 1978, when the submarine lead acid batteries will also be replaced by a flywheel generator.

2.27 A He-Ne laser interferometer for Tokamak electron density measurements

(P. Nielsen)

A new system was developed for measuring line densities in Tokamaks. It is based on the system reported by Weisberg (1972). An Ashby-Jephcott He-Ne laser-coupled cavity system operated at 3.39 μm is feedback stabilized against mechanical motion before measurement. The feedback loop is broken immediately before measurement. The system gives a linear response to plasma line density for fringe shifts between 1/100 and 1/10 of a fringe (sensitivity - $3 \cdot 10^{14}$ cm^{-2}). With the feedback loop open, the system is also sensitive to mechanical vibrations, limiting the useful period to ∿ 500 μs.

In the new system, use is made of the different sensitivities of the 3.39 and 0.63 μm lines. The laser lases alternately at the two wavelengths at a frequency of 2-10 kHz. Feedback stabilization is switched on when the red line is transmitted and broken when the infrared line is on.

2.28 References (see also 5.2)

ANDERSEN, H.H., LENSKJÆR, T., SIDENIUS, G., and SØRENSEN, H. (1976). J. Appl. Phys. 47, 13-16.

ANDERSEN, V., NIELSEN, P., and SILLESEN, A.H. (1976). Risø Report No. 352, 55-57.

CHRISTOFFERSEN, G.B., JENSEN, V.O., and MICHELSEN, P. (1974). Phys. Fluids 17, 390-399.

HILDEBRANDT, D. and MANNS, R. (1976). Phys. Stat. Sol. (a) 38, K155-K157.

HOLMÉN, G., SVENSSON, B., and BURÉN, A. (1977). Proceedings of the 7th International Conference on Atomic Collisions in Solids. (Moscow, September 1977). To be published.

JENSEN, V.O. and MICHELSEN, P. (1972). Risø Report No. 257.

JENSEN, V.O. (1976). Risø Report No. 322.

JØRGENSEN, L.W., SILLESEN, A.H., and ØSTER, F. (1975). Plasma Physics 17, 453-461.

LEVINE, A.M. and KUCKES, A.F. (1966). Phys. Fluids 9, 2263-2266.

LITTMARK, V. and MADERLECHNER, G. (1976). Proceedings of the 7th Yugoslav Symposium on the Physics of Ionized Gases, Dubrovnik 1976, 139-142.

MOTLEY, R.W. and D'ANGELO, N. (1963). Phys. Fluids 6, 296-299.

OEN, O.S. and ROBINSON, M.T. (1976a). J. Nucl. Mat. 63, 216-214.

OEN, O.S. and ROBINSON, M.T. (1976b). Nucl. Instr. Meth. 132, 647-653.

ROBINSON, J.E. (1974). Rad. Eff. 23, 29-36.

ROBINSON, J.E., KWOK, K.K., and THOMPSON, D.A. (1976). Nucl. Instr. Meth. 132, 667-671.

SATO, N., SUGAI, H., and HATEKEYAMA. (1977). Plasma Phys. 19, 187-207.

SIDENIUS, G. and LENSKJÆR, T. (1976). Nucl. Instr. Meth. 132, 673-678.

SIGMUND, P. (1969). Phys. Rev. 184, 383-416.

SØRENSEN, H. (1977). J. Appl. Phys. 48, 2244-2251.

SØRENSEN, H. (1977). Proceedings of the International Symposium on Plasma Wall interaction. Julich, October 1976. (Pergamon Press, Oxford), 437-441.

SØRENSEN, H. (1976). Appl. Phys. 9, 321-329.

VUCANIC, J. and SIGMUND, P. (1976a). Proceedings of the 7th Yugoslav Symposium on the Physics of Ionized Gases, Dubrovnik 1976, 134-138.

VUCANIC, J. and SIGMUND, P. (1976b). Appl. Phys. 11, 265-272.

WEISBERG, K.-V. (1972). Proceedings of the 7th Symposium on Fusion Technology, Grenoble, France, October 1972. EUR 4938e, 51-57.

3. METEOROLOGY

The meteorology section is primarily engaged in studies of the planetary boundary layer. The theoretical and experimental work can be roughly classified as follows: micrometeorological research (3.1-3.3), climatological investigations, development of meteorological instruments (3.4-3.6), and applied meteorology (3.7).

At Risø a 120 m tower is available for experimental work. Meteorological variables such as wind speed and direction, temperature and humidity are measured routinely at a number of heights. As a result of the measurements, data records are available containing 19 years of hourly readings. These records are used extensively both by the section and by other groups.

For field experiments, there are a 50 m mobile tower, a data acquisition system installed in a van, and a telemetry system. The digital data system is capable of sampling 60 signals simultaneously at a rate of 200 times per second, and the telemetry system can transmit 32 channels over essentially line-of-sight distances up to more than 50 km at a rate of 25000 8-bit numbers per second.

Micrometeorological research aims at descriptions of the structure of atmospheric turbulence and its dependence on external parameters, such as surface characteristics and the synoptic weather situation. An important goal is parameterization of the transport properties of atmospheric turbulence, so that the planetary boundary layer can be realistically incorporated in numerical weather prediction schemes. Work on numerical and physical improvements of boundary layer models was continued (3.2).

The experimental study of the influence of abrupt changes in surface roughness on the flow immediately above the surface was carried out on the Bognæs site in Roskilde fjord until the end of the year (3.1). Turbulence measurements were performed during periods with favourable weather conditions. Efforts in the field of air-sea-interaction was primarily concentrated on the analysis of the data obtained during the Joint North Sea Wave Project (JONSWAP 1975). Further, the equipment developed for the JONSWAP experiment was used in two experiments at Lake Washington, USA (3.3).

Climatological investigations mainly concern the analysis of data collected on Greenland, and at Risø and other locations in Denmark. The section now operates about 18 automatic observatories, of which 6 in North Greenland are operated jointly with the Danish Meteorological Institute.

Work was continued on the development and testing of meteorological instruments and equipment (3.4-3.6). Of special interest is the continuous operation at Risø of a monostatic acoustic sounder where the Doppler shifted returned signal is used to display the vertical velocity in the lowest 1000 m of the atmosphere.

Tasks of an applied nature are now taking up a larger share of the section's time, because of an increase in contractual work. These tasks include: site evaluation for nuclear power stations and dispersion modelling, air pollution studies, evaluation of dynamic effects of wind on engineering structures, development and testing of meteorological instruments, and evaluation of wind power as an alternative energy source.

The section is a member of the Gedser Test Group which is a subcontracter to DEFU (Research Association of the Danish Electricity Suppliers). The Gedser Test Group is responsible for carrying out a series of experiments on the Gedser wind turbine in order to establish a set of data for comparative analyses between this turbine and the new US wind turbines. The 200 kW Danish Gedser wind turbine is the only older large wind turbine still in existence.

The section entered into a five year contract with the agency responsible for the initial planning of the building of a bridge over the Great Belt. The first phase of the contract was put into operation in September with meteorological measurements along a 70 m high mast errected at Sprogø, a small island in the middle of the Belt. The purpose of the measurements during the first phase is to obtain a set of data which can supplement the Danish wind codes. In subsequent phases it is planned to carry out turbulence measurements in order to evaluate the dynamic effects on the bridge of the windfield over the Belt.

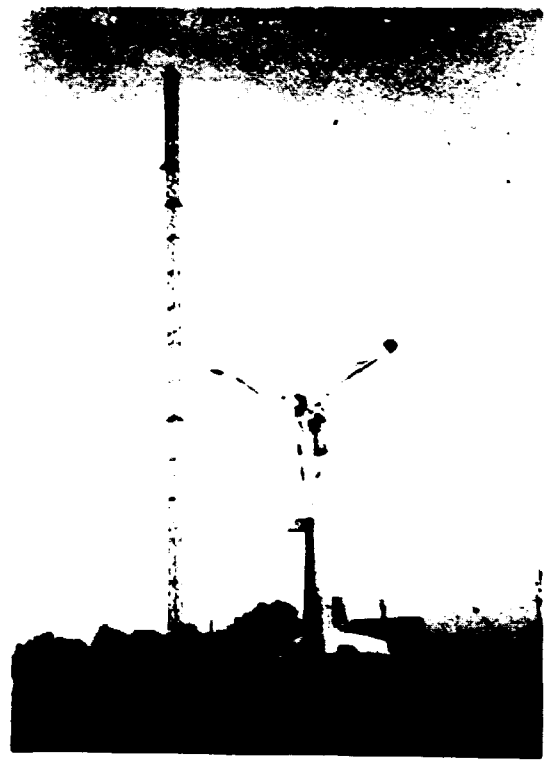

Fig. 28 The Gedser wind turbine and the mobile meteorological tower seen from the west. The tower is situated 30 m west of the turbine. The usual meteorological instruments and sonic anemometers are mounted in the tower. Data are transmitted from the rotor to the ground by means of a telemetry system, while the ground fixed measurements are recorded by a data acquisition system installed in a van. The tower, the telemetry system and the data system in the van are the core of the field experiment equipment.

3.1 Flow over non-uniform terrain

(N.O. Jensen, N.E. Busch, E.W. Peterson (Oregon State University, Oregon, USA), J. Højstrup, and C.J. Christensen)

The joint Risø-Oregon State University investigation of flow over a change in terrain roughness was continued at the Bognæs site. The main advantage of this site over the previous one on the north shore of the Risø peninsula (Peterson et al. 1976) is that it is nearly flat. As in the previous experiment, the change in surface-roughness between water and land is utilized. Measurements were carried out along 3 masts positioned approximately in a line at 0 m, 82 m, and 160 m from the coastline. Each mast was instrumented with six cup-anemometers, a wind-

direction sensor, and two thermometers. Measurements were recorded as 10 minute averages on Aanderaa dataloggers. The surface roughness length has been found to change by approximately three orders of magnitude.

Turbulence measurements were carried out at the same site during selected periods. The middle mast was then additionally instrumented with 6 hot-wire anemometers. All 18 cup and 6 hot-wire anemometers involved were sampled at a high rate and the data were transmitted to Risø by telemetry. The hot-wires made it possible to measure wind variance at frequencies well into the inertial subrange, and hence to estimate dissipation rates of turbulent energy. The measurements were subject to detailed analysis and were compared to a theoretical model (Peterson 1969). Agreement between measurements and theory is excellent. A report on the results is in progress (Peterson et al. 1978).

The experimental set-up at the Bognæs site is now dismantled after two years of operation, and the results of the routine measurements have been reported (Jensen and Peterson 1977). Funds were obtained to continue the study of the effect of terrain changes. The equipment used in the two previous studies will be re-erected at its first location for the joint experiment Risø-78, which is being planned in cooperation with Pennsylvania State University and Oregon State University. This study will emphasize the effect of change in surface elevation on such quantities as surface heat and momentum fluxes.

It was shown that miscellaneous theories for flow over low ridges give mutually consistent results, and that these results can be used to quantify certain features of the wind profile downwind from an escarpment (Jensen and Peterson 1978). In agreement with results of the stress-profile experiments at Risø (Jensen 1978a), it was theoretically shown that a rather substantial drop in the stress can be expected within an accelerating flow (Jensen 1978b). Further information about the vertical structure of turbulence may be deducted from the Risø-78 experiment.

In an attempt to show how non-uniform terrain affects the flow on a larger scale, a theoretical study was made on the response of the planetary boundary layers to a change in surface rough-

ness (Jensen 1978c). The ratio between upstream and far downstream surface friction velocities relative to a change in surface roughness is given on the basis of results from surface Rossby-number similarity theory. By means of simple theories for the internal boundary layer, which are found to compare quite well with recent numerical results from higher order closure models, it is found that even at a downwind distance where the internal boundary layer has grown to the full height of the planetary boundary layer, the surface stress still considerably exceeds the equilibrium value.

3.2 Numerical modelling of the planetary boundary layer

(I. Troen, N.E. Busch, and C.J. Christensen)

Work was done on the numerical improvement of the boundary layer model (Busch et al. 1976) to make it more efficient for use in mesoscale models. The original forward-time extrapolation scheme, which requires very small time steps to be stable (down to less than 10 s in this model), was abandoned in favour of an implicit Crank-Nicholson scheme, that is stable and accurate for time steps up to 10-20 times larger. Some experiments with different vertical resolution showed that with the simple centered difference scheme for the calculation of the spatial derivatives the requirement to resolution is very high. A version of the model was coded which employs a Galerkin variational technique with piecewise linear basic functions. Preliminary results indicate that this method is superior in numerical accuracy, and not more expensive with respect to computing time.

3.3 Air-sea interaction

(S.E. Larsen, N.E. Busch, N.O. Jensen, K. Katsaros*, S. Stage*, S.J.S. Kalsa* (* University of Washington, Washington, USA), and R.M. Williams (Argonne National Laboratory, Illinois, USA))

Analysis of data from the JONSWAP 1975 experiment is in progress. Further, the group was involved in the analysis of data gathered in the air mass modification and transformation experiment (AMTEX) during cold air out-breaks from continental China to the East China Sea.

Otherwise efforts in connection with air-sea interaction were largely concentrated on experimental work. The equipment used

Fig. 29 DMSP satellite imagery at 1136 JST (Japanese Standard time) 17 February 1975 from the East China Sea region. Part of the Korean peninsula is seen in the upper part of the picture. The hexagon marks the AMTEX (see 3.3) (Air Mass Transformation Experiment) observational network, the goal of which is to describe the processes by which momentum, heat and moisture are exchanged between ocean and atmosphere.

This particular region was chosen because of the large air-sea temperature contrasts present here when cold continental air masses flow southward and meet the warm Kuroshio (Japanese current). The consequence is vigorous convection. The clouds in the central part of the picture, with the exception of the vortex cloud street developing downwind from Cheju Island, result from such convective motions. It is found that the convection is organized in mesoscale cellular patterns.

in JONSWAP 1975 (Busch and Larsen 1975) was used in two experiments at Lake Washington, Washington, USA. The purpose of the first experiment was in part to study the relation between production and dissipation of temperature variance over water, especially in connection with plumes of high turbulence intensity; in part to study the behaviour of the high-frequency velocity and temperature fields at various heights over the water. The purpose of the second experiment was to study the correlation between the turbulent fluxes measured close to the water surface (50 cm) and surface variables such as the high-frequency wavefield and the water surface temperature (McIntosh et al. 1975).

3.4 Quantitative sodar measurements of atmospheric turbulence

(D.W. Thomson and L. Kristensen)

Both the turbulent energy dissipation rate, ε, and the rate of destruction of turbulent temperature fluctuations, N, may in many situations be derived remotely from sodar measurements (Neff 1975, Gaynor 1977, and Caughey et al. 1978). Determination of ε and N from the sodar-determined temperature and velocity structure parameters C_T^2 and C_v^2, respectively, is performed on the basis of similarity arguments developed by Wyngaard et al. (1971) and by Kaimal (1973).

In experiments at the Pennsylvania State University (PSU), the estimates of ε and N in the convectively unstable boundary layer, in stable layers several hundred meters above the ground (Thomson et al. 1978), and in power plant cooling tower plumes were made solely on the basis of signal amplitude measurements. Corrections for the complicated bistatic system geometry were made using the techniques developed by Thomson and Coulter (1974) and by Coulter (1976). Recently, an improved generalized analysis of the bistatic geometry was completed.

Gaynor (1977) employed an alternative technique for estimating ε based on determination of the structure parameter from signal Doppler shifts. Fast Fourier Transform software for computing

Doppler spectra in the PSU sodar minicomputer was completed and thoroughly tested.

Experimental sodar studies at Risø during 1977 were limited to calibration, and test and evaluation of the new monostatic Sensitron system. Theoretical work was directed toward the development of experimental techniques for optimum application of sodar to meteorological measurements problems in complex terrain situations. Analysis indicates that vertical stability and wind profiles derived from sodar, particularly in complex terrain during stable atmospheric conditions, will be far better for evaluative studies of numerical dynamical models than the few existing pibal, tetroon and tracer measurements.

3.5 A phase-locked loop, continuous wave, sonic anemometer-thermometer

(S.E. Larsen, F. Weller*, and J.A. Businger*, (* University of Washington, Washington, USA))

A new principle for sonic anemometry was developed. In this system the magnitude of the acoustic transmission time across the path length is retrieved as a frequency variation by means of an integrated monolithic, phase-locked loop (Larsen et al. 1977). The main advantage of the instrument is that the acoustic path-length does not enter the calibration equation, and that wind speeds are obtained without contamination from variations in the sound velocity.

3.6 Measurements of high-frequency temperature fluctuations

(S.E. Larsen, J. Højstrup, and C. Gibson (University of California, La Jolla, California, USA))

A new temperature bridge for measurements of high frequency temperature fluctuations was developed. The bridge is an ac-bridge with a carrier frequency of 50 kHz and an electronic noise contribution equivalent to the thermal noise of an ideal 33 Ω resistor.

Furthermore, a study was made of techniques and problems involved in measurements of turbulent temperature fluctuations over the ocean (Larsen et al. 1978). This review summarizes the relevant sensor parameters in relation to resolution, response, and signal contamination by velocity and radiation variations.

Special attention was paid to the problems associated with salt contamination of the sensor and the resulting contamination of the temperature signal by humidity fluctuations.

3.7 Dynamic windloading

(O. Christensen (Technical University of Denmark), M. Nansen-Nielsen (Vølund A/S), and S. Frandsen)

From March 1976 until May 1977 a field experiment concerning cross-wind excitation of steel chimneys was carried out by the Technical University, Risø, and the steel chimney manufacture Vølund A/S. It was financially supported by the Danish Technological Council.

The experiments were performed to investigate the vibrations that occur when the frequency of the alternating vortex shedding equals the natural frequency of the structure. For most steel chimneys such resonance occurs at common wind speeds. This effect usually determines the design load. Measurements were made on five chimneys at various sites in Denmark. The sites were selected so that different terrain categories were represented. Parameters such as height, diameter and internal structure also differed for the five chimneys.

In the Danish wind code it is proposed that the magnitude of the logarithmic decrement (a measure of the damping of the structure) be chosen in the interval $0.03 < \delta < 0.07$. The present experiments have shown that, for simple structures, the decrement can be as low as 0.015 - hence the wind code value is not a conservative estimate (the larger is δ, the smaller are the amplitudes).

To further compare the results with the wind code, a so-called equivalent lift-coefficient was calculated. The lift-coefficient is a number that transforms the dynamic loads into an equivalent static load. The analysis indicated that the wind code overestimates this quantity by at least a factor of two. Hence, the code is very conservative in this case.

3.8 References (see also 5.2)

BUSCH, N.E., CHANG, S.W., and ANTHES, R.A. (1976). J. Appl. Meteorol. 15, 909-919.

BUSCH, N.E. and LARSEN, S.L. (1975). Risø Report No. 334, 68-70.

CAUGHEY, S.J., CREASE, B.A., ASIMOKOPOULOS, D.N., and COLE, R.S. (1978). Quantitative bistatic acoustic sounding of the atmospheric boundary layer, Quart. J. Royal Meteorol. Soc. In the press.

COULTER, R.L. (1976). System geometry and the interpretation of sodar data. PhD. Thesis, The Pennsylvania State University, Pennsylvania, USA.

GAYNOR, J.E. (1977). Appl. Meteorol. 16, 148-155.

JENSEN, N.O. and PETERSON, E.W. (1977). Wind Flow near the surface over nonuniform terrain. Technical report, available from Physics Department, Meteorology Section, Risø National Laboratory.

JENSEN, N.O. (1978a). Risø Report No. 330. In preparation.

JENSEN, N.O. (1978b). Simultaneous measurements over land and water. Accepted for publication in Bound. Layer Meteorol.

JENSEN, N.O. (1978c). Change of surface roughness and planetary Boundary layer. Quart. J. Roy. Meteorol. Soc. 109, 351-356.

JENSEN, N.O. and PETERSON, E.W. (1978). On the escarpment wind profile Accepted for publication in Quart. J. Roy. Meteorol. Soc.

KAIMAL, J.C. (1973). Bound. Layer Meteorol. 4, 289-309.

LARSEN, S.E., WELLER, F., and BUSINGER, J.A. (1977). A phase-locked loop continuous wave sonic anemometer-thermometer. Submitted for publication in J. Appl. Meteorol.

LARSEN, S.E., HØJSTRUP, J., and GIBSON, C. (1978). Measurements of high frequency temperature fluctuations over the ocean. To appear in "Instruments and Methods in Air Sea Interaction" Ed. L. Hasse.

McINTOSH, D.A., Street, R.L., and HSU, E.Y. (1975). Geophys. Research Letters 2, 12-14.

NEFF, W.D. (1975). NOAA Tech. Rept. ERL 322-WPL 38, 34.

PETERSON, E.W. (1969). Quart. J. Roy. Meteorol. Soc. 95, 561.

PETERSON, E.W., KRISTENSEN, L., and SU, C.C. (1976). Quart. J. Roy. Meteorol. Soc. 102, 857-869.

PETERSON, E.W., JENSEN, N.O., and HØJSTRUP, J. (1973). Observations of downwind development of wind speed and variance profiles at Bognæs, and comparison with theory. To be published.

THOMSON, D.W. and COULTER, R.L. (1974). J. Geophys. Res. 79, 5541-5549.

THOMSON, D.W., COULTER, R.L., and WARHAFT, Z. (1978). Simultaneous measurements of turbulence in the lower atmosphere using sodar and aircraft. Accepted for publication in J. Appl. Meteorol.

WYNGAARD, J., IZUMI, J., and COLLINS, S.A., Jr. (1971). J. Opt. Soc. Am. 61, 1646-1650.

4. LIQUID N_2 AND He PLANT

The production of liquid N_2 and He amounted to 200000 and 19000 litres,respectively. Out of these amounts, 10000 litres of liquid He were delivered to laboratories in Copenhagen, Odense and Århus.

5. EDUCATIONAL ACTIVITIES AND PUBLICATIONS

5.1 Lectures

ALS-NIELSEN, J., Mean field theory, the Ginzburg criterion and marginal dimensions.
1) Chalk River Nuclear Laboratories, Canada, (March).
2) Boston University, Massachusetts, USA, (April).
3) Brandeis University, Massachusetts, USA, (April).
4) Harward University, Massachusetts, USA, (May).

BJERRUM MØLLER, H., Neutron scattering investigation of the mixed valence system Thulium Selenide. Oak Ridge National Laboratory, Tennessee, USA, (July).

BURAS, B. and CARNEIRO, K., Selected topics in neutron and X-ray scattering (lecture series). University of Copenhagen, (spring semester).

BURAS, B. and CARNEIRO, K., Scattering techniques in the physics of condensed matter (lecture series). University of Copenhagen, (autumn semester).

CHANG, C.T., Slowing-down of alpha-particles in thermonuclear plasmas and the problem of pellet ablation. Max-Planck Institute of Plasma Physics, Garching, F.R.G., (July).

CHRISTENSEN, O. (and LARSEN, S.E.), Vindmåling ved og nær jordens overflade. (Wind measurements at and near the earth's surface). Meteorological Institute, Copenhagen, (October).

JENSEN, N.O., The growth of mixed layers and entrainment. Niels Bohr Auditorium, Risø, (February).

JENSEN, N.O., Turbulence in non-homogeneous flow. University of Washington, Washington, USA, (April).

JENSEN, N.O., Sonic anemometry. Naval Postgraduate School, Monterey, California, USA, (July).

JENSEN, N.O., Penetrative convection. Pennsylvania State University, Pennsylvania, USA, (September).

JENSEN, N.O., Koherensforhold i den naturlige vind. (Coherence conditions in the natural wind). Technical University of Norway, Trondheim, Norway, (December).

JENSEN, N.O., Fusions energiens muligheder. (The possibilities of fusion energy). Niels Bohr Auditorium, Risø (April).

JENSEN, N.O., Fusions energiens problemer og udsigter. (Problems and possibilities of fusion energy). Niels Bohr Auditorium, Risø, (June).

JENSEN, V.O., Fusions energi. (Fusion energy). Odense Seminarium, Odense, (September).

LARSEN, S.E., Theory and practice in spectral analysis (lecture series). University of Washington, Washington, USA, (July).

LARSEN, S.E., Dynamic and static calibration problems for hot-wires and cold-wires. Fluid Mechanics and Heat Transfer Group, Seattle, Washington, USA, (March).

LARSEN, S.E., Flux determination by use of the dissipation method (lecture series). University of Washington, Washington, USA, (August).

LARSEN, S.E., Three-dimensional hot-wire measurements of atmospheric surface layer turbulence. Naval Postgraduate School, Monterey, California, USA, (September).

LARSEN, S.E., Principle of operation of a phase-locked loop sonic. Wave Propagation Laboratory, Boulder, Colorado, USA, (September).

LARSEN, S.E., Working program of the meteorology section at Risø. Argonne National Laboratory, Illinois, USA, (September).

LARSEN, S.E. (and BUSCH, N.E.), Analysis of hot- and cold-wire data from the Kansas 1968-Experiment.
1) University of Washington, Washington, USA, (November 1975).
2) Oregon State University, Oregon, USA, (June).

LARSEN, S.E. (and PETERSEN, E.L.), Statistical analysis of 700 000 years paleo temperature series. University of Washington, Washington, USA, (October 1976).

LARSEN, S.E., (WELLER, F., and BUSINGER, J.A.), The working principle of Fred Weller's sonic. University of Washington, Washington, USA, (April).

LINDGÅRD, P.-A., Magnetic properties of rare earth and rare earth transition metal alloys.
1) Institute Laue-Langevin, Grenoble, France, (March).
2) Imperial College, London, U.K., (July).

LINDGÅRD, P.-A., Spin waves in strongly anisotropic magnets. Institut Laue-Langevin, Grenoble, France, (March).

LINDGÅRD, P.-A., Excitations and spin waves. AERE, Harwell, U.K., (July).

MACKENZIE, G.A., Studies of molecular crystals by neutron and Raman scattering. Technical University of Denmark, Lyngby, (March).

MACKENZIE, G.A., Neutron powder diffraction and constrained refinement.
1) University of Aarhus, Aarhus, (March).
2) H.C. Ørsted Institute, Copenhagen, (November).

MØLLENBACH, K., Undersøgelse af biologiske strukturer ved hjælp af neutronspredning. (Investigation of biological structures by means of neutron scattering). Panum Institute, Copenhagen, (January).

NIELSEN, M., Sturctures, dynamics and magnetics of adsorbed layers on graphite. H.C. Ørsted Institute, Copenhagen, (March).

NIELSEN, P., Pellet refuelling. University of Texas at Austin, Texas, USA, (November).

PÉCSELI, H.L., University of Tromsø, Norway, (October).
1) Interaction between electron plasma waves and ion acoustic waves.
2) Turbulent fluctuations in the ionosphere.

PETERSEN, E.L. (and CHRISTENSEN, J.), New emphasis on battle-field visibility control: The dynamics of smoke clouds. Advisory Group for Aerospace Research and Development (AGARD), annual meeting, Copenhagen, (September).

PETERSEN, E.L. (and LARSEN, S.E.), Stochastic model building for discrete time series applied on a paleo temperature series from the last 700 000 years. Pennsylvania State University, Pennsylvania, USA, (November).

SKRIVER, H.L., Self-consistent energy bands for ordered alloys. National Research Council, Ottawa, Canada, (August).

SKRIVER, H.L., Magnetic properties of transition metal alloys from a self-consistent band theory. Vrie Universiteit, Amsterdam, The Netherlands, (November).

THOMSON, D.W., Atmospheric turbulence and wind measurements using sodar. Royal Netherlands Meteorological Institute, The Netherlands, (October).

THOMSON, D.W., Seeing the atmosphere with sound. Technical University of Denmark, Lyngby, (November).

5.2 Publications

ALS-NIELSEN, J. and BIRGENAU, R.J. (1977). Mean field theory, the Ginzburg criterion, and marginal dimensionality of phase transitions. Am. J. Phys. 45, 554-560.

ALS-NIELSEN, J., BIRGENAU, R.J., KAPLAN, M., LITSTER, J.D., and SAFINYA, C.R. (1977). Experimental observation of anomalous ordering in a Landau-Peierls system. Phys. Rev. Lett. 39, 352-355.

ALS-NIELSEN, J., KJEMS, J.K., BUYERS, W.J.L., and BIRGENAU, R.J. (1977). Critical scattering in the singlet-ground state system Pr_3Tl. Physica B+C 86-88, 1162-1163.

ALS-NIELSEN, J., KJEMS, J.K., BUYERS, W.J.L., and BIRGENAU, R.J. (1977). Observation of a central mode in an exchange-coupled singlet-ground state system, J. Phys. C: Solid State Phys. 10, 2673-2678.

BIRGENAU, R.J., ALS-NIELSEN, J., and SHIRANE, G. (1977). Critical behaviour of pure and site-random two dimensional antiferromagnets. Phys. Rev. B16, 280-292.

BJERRUM MØLLER, H., SHAPIRO, S.M., and BIRGENAU, R.J. (1977). Field-dependent magnetic phase transitions in mixed-valent TmSe. Phys. Rev. Lett. 39, 1021-1025.

BURAS, B., NIIMURA, N., and STAUN OLSEN, J. (1977). Optimum resolution in X-ray energy-dispersive diffractometry. Physics Laboratory II, University of Copenhagen, Monograph No. 77-19, 7 pp.

BURAS, B., KOFOED, W., LEBECH, B., and BÄCKSTRÖM, G. (1977). A high-pressure cell for neutron crystal spectrometry. Risø Report No. 357, 32 pp.

BURAS, B., STAUN OLSEN, J., and GERWARD, L. (1977). White beam X-ray energy-dispersive diffractometry using synchrotron radiation. Physics Laboratory II, University of Copenhagen, Monograph No. 77-24, pp. 7 pp.

BURAS, B., STAUN OLSEN, J., and GERWARD, L. (1977). X-ray energy-dispersive diffractometry using synchrotron radiation. In: Synchrotronstrahlung bei DESY, ein Handbuch für Benutzer. Edited by E.E. Koch and C. Kunz, Hamburg 1977, 286-290.

BURAS, B., STAUN OLSEN, J., GERWARD, L., WILL, G., and HINZE, E. (1977). X-ray energy-dispersive diffractometry using synchrotron radiation. J. Appl. Cryst. 10, 431-438.

BUSCH, N.E. (1977). Fluxes on the surface boundary layer over the sea. In: Modelling and prediction of the upper layers of the ocean. Edited by E.B. Kraus (Pergamon Press), Oxford, 72-91.

CARNEIRO, K. (1977). Neutron scattering from ^{36}Ar and ^{4}He films. Journal Physique 38, Collogue C4, 1-8.

CARNEIRO, K., ELLENSON, W.D., PASSELL, L., McTAGUE, J.P., and TAUB, H. (1976). Neutron scattering study of the structure of adsorbed helium monolayers and of the excitation spectrum of few-atomic-layer superfluid films. Phys. Rev. Lett. 37, 1695-1698.

CARNEIRO, K., HESSEL ANDERSEN, N., KJEMS, J.K., and VOGT, O. (1977). Critical behaviour of the magnetization in TbSb and $Tb_{0.6}Y_{0.4}Sb$. In: Crystal Field Effects in Metals and Alloys. Edited by A. Furrer (Plenum Press), New York, 99-103.

CHANG, C.T. (1977). On the use of Langmuir probes in a laser-produced plasma. IPP 4/150, 27 pp.

CHANG, C.T. and HASHMI, M. (1977). Oscillation modes of a laser-produced plasma expanding into a uniform magnetic field. Phys. Fluids 20, 533-535.

CHANG, C.T., HASIMI, M., and PANT, H.C. (1977). Study of a laser-produced plasma by Langmuir probes. Plasma Phys. 19, 1129-1138.

COOKE, J.F. and LINDGÅRD, P.-A. (1977). Canonical transform method for treating strongly anisotropic magnets. Phys. Rev. B16, 408-418.

DUTTON, J.A., KERMAN, B.K., and PETERSEN, E.L. (1976). Contributions to the simulation of turbulence. NASA-CR-2762, 270 pp.

DYSTHE, K.B. and PÉCSELI, H.L. (1977). Non-linear Langmuir wave modulation in collisionless plasmas. Plasma Phys. 19, 931-943.

ELLENSON, W.D. and KJEMS, J.K. (1977). Soft phonon and central peak scattering in a molecular crystal system: $C_6Cl_4O_2$. J. Chem. Phys. 67, 3619-3623.

FISCHER, P., MEIER, G., HÄLG, W., LEBECH, B., RAINFORD, B.D., and VOGT, O. (1977). Magnetic phase transitions of CeSb: Results of structure refinements. Risø Report No. 369, 28 pp.

HEDEMANN JENSEN, P., PETERSEN, E.L., THYKIER-NIELSEN, S., and HEIKEL VINTHER, F. (1977). Calculation of the individual and population doses on Danish territory resulting from hypothetical core-melt accidents at the Barsebäck Reactor. Risø Report No. 356, 118 pp.

HOLTHAM, P.M., JAN, J.-P., and SKRIVER, H.L. (1977). Band-structure of Thallium by the LMTO method. J. Phys. F: Metal Phys. 7, 635-646.

HOUMANN, J.G., LEBECH, B., MACKINTOSH, A.R., BUYERS, W.J.L., McMASTERS, O.D., and GSCHNEIDNER, K.A. Jr. (1977). Central peaks and soft modes in Praseodymium. Physica B+C 86-88, 1156-1157.

HØJSTRUP, J., RASMUSSEN, K., and LARSEN, S.E. (1977). Letter to the editor: Dynamic calibration of temperature wires in moving air. DISA-Information No. 21, 33.

JAN, J.-P. and SKRIVER, H.L. (1977). Band structure and Fermi surface of Cu_2Sb by the LMTO method. J. Phys. F: Metal Phys. 1, 957-967.

JAN, J.-P. and SKRIVER, H.L. (1977). Relativistic band structure and Fermi surface of $PdTe_2$ by the LMTO method. J. Phys. F: Metal Phys. 7, 1719-1730.

JENSEN, N.O. and HJORTH-HANSEN, E. (1977). Dynamic excitation of structures by wind: Turbulence and response measurements at Sotra Bridge. SINTEF, Division of Structural Engineering, Trondheim,

JENSEN, V.O. (1977). JET vedtaget efter 10 års forsinkelse (JET accepted after ten years' delay). Ingeniørens Ugeblad No. 44, November 4, 6-7.

JENSEN, V.O. (1977). Havet kan løse alle energiproblemer (The sea can solve all energy problems - newspaper article). Aftenavisen Roskilde Tidende, November 26.

JENSEN, V.O. (1977). JET-projektet vigtigt skridt mod praktisk udnyttelse af EF-landenes fusionsforskning (JET, a step towards the practical use of fusion research in EC countries). Europa No. 9, November 4-6.

JENSEN, V.O. (1977). Kendsgerninger om fusionsenergi (Facts about fusion energy - newspaper article). Roskilde Tidende, June 6.

JUUL RASMUSSEN, J. (1977). Nonlinear electron plasma waves in a cylindrical wave guide. Risø-M-1911, 34 pp.

JUUL RASMUSSEN, J. (1977). Pulsudbredelser og instabiliteter i et ion-beam-plasma system og vekselvirkning mellem elektron-plasma bølger og ion-akustiske bølger (Pulse propagation and instabilities in an ion-beam-plasma system and interaction between electron-plasma waves and ion acoustic waves). Risø-M-1950, 77 pp.

KJEMS, J.K. (1977). Neutron scattering studies of the cooperative Jahn-Teller effect. In: Electron-Phonon Interaction and Phase Transitions. Edited by T. Riste, (Plenum Press), New York. NATO Advanced Studies Series B: Physics 29, 302-322.

KJEMS, J.K. (1977). The cooperative Jahn-Teller effect studied by neutron scattering. In: Crystal Field Effects in Metals and Alloys. Edited by A. Furrer (Plenum Press), New York, 174-84.

KOFOED-HANSEN, C. (1977). Unsolved problems in nuclear physics. Nature 226, 117.

KOFOED-HANSEN, O. (1977). Why do we study nuclear physics? Progress in Scientific Culture 1, 375-381.

KOWALSKA, A. and LINDGÅRD, P.-A. (1977). Bose operator expansion of tensor operators in the theory of magnetism. Physica B+C 86-88, 1111-1112.

LINDGÅRD, P.-A. (1977). Spin waves in anisotropic magnets. In: Crystal Field Effects in Metals and Alloys. Edited by A. Furrer (Plenum Press), New York, 9-18.

LINDGÅRD, P.-A. (1977). Spin wave theory of strongly anisotropic magnets. Physica B+C 86-88, 53-54.

LINDGÅRD, P.-A. (1977). Theory of rare-earth alloys. Phys. Rev. B16, 2168-2176.

MACKENZIE, G.A., ARTHUR, J.W., and PAWLEY, G.S. (1977). The structural phase transition in octafluornaphthalene. J. Phys. C: Solid State Phys. 10, 1133-1149.

MACKENZIE, G.A., BURAS, B., and PAWLEY, G.S. (1977). The structure of octafluoronaphthalene at high pressures investigated by neutron powder diffraction. Physics Laboratory II, University of Copenhagen, Moncgraph No. 77-30, 10 pp.

MACKENZIE, G.A., PAWLEY, G.S., and DIETRICH, O.W. (1977). Phonon measurements and model calculations for Naphthalene-d_8. J. Phys. C: Solid State Phys. 10, 3723-3725.

MACKINTOSH, A.R. (1977). The magnetism of rare earth metals. Physics Today 30, 23-30.

MAHRT, L. and JENSEN, N.O. (1977). Comments on "Penetrative convection due to a field of thermals" by M.J. Manton (J. Atmos. Sci. 32, 2272-2277, 1975), J. Atmos. Sci. 34, 432-433.

MICHELSEN, P., PÉCSELI, H.L., and JUUL RASMUSSEN, J. (1977). Ion acoustic waves in the presence of electron plasma waves. Phys. Lett. 59A, 445-447.

MICHELSEN, P., PÉCSELI, H.L., and JUUL RASMUSSEN, J. (1977). Ion-beam-excited electrostatic ion-cyclotron instability. Phys. Fluids 20, 866-867.

MICHELSEN, P., PÉCSELI, H.L., JUUL RASMUSSEN, J., and SATO, N. (1977). Stationary density variation produced by a standing plasma wave. Fluids 20, 1094-1096.

MØLLENBACH, K., KJEMS, J.K., and SMITH, S.H. (1977). Gamma-ray diffraction studies of the mosaic distribution in $TmAsO_4$ near the cooperative Jahn-Teller transition at 6 K. In: Electron-Phonon Interaction and Phase Transitions. Edited by T. Riste, (Plenum Press), New York, NATO Advanced Studies Series B: Physics 29, 323-326.

NIELSEN, M. and McTAGUE, J.P. (1977). Antiferromagnetic structure in adsorbed O_2 monolayers. Physica B+C 86-88, 675-676.

NIELSEN, M., McTAGUE, J.P., and ELLENSON, W.D. (1977). Adsorbed layers of D_2, H_2, O_2 and ^3He on graphite studied by neutron scattering. Journal Physique 38, Colloque C4, 10-18.

PAWLEY, G.S., MACKENZIE, G.A., and DIETRICH, O.W. (1977). Neutron powder diffraction and constrained refinement. The structure of p-dibromo and p-diiodotetrafluorobenzene. Acta Cryst. A33, 142-145.

PETERSEN, E.L. and JENSEN, N.O. (1977). Notat om meteorologiske forhold vedrørende placering af større el-producerende vind-kraftanlæg (Note on meteorological conditions relevant to site evaluation of large-scale electricity-producing wind-power plants). Kontraktrapport til Handelsministeriet og De Danske Elværkers Vindkraftprojekt. 13 pp.

PETERSEN, E.L. and JENSEN, N.O. (1977). Reply to comments of Hall and Neff on the note "A mesoscale phenomenon revealed by an acoustic sounder". (J. Appl. Meteorol. 15, 661, 662-664, 1976), J. Appl. Meteorol. 16, 110-11.

PETERSEN, E.L. and LARSEN S.E. (1977). Stochastic model building for discrete time series applied on a paleo temperature series from the last 700 000 years. Proceedings of the Fifth Conference on Probability and Statistics in Atmospheric Sciences, American Meteorological Society, Las Vegas, Nevada, 303-307.

RAINFORD, B.D., BUPAS, B., and LEBECH, B. (1977). Inelastic neutron scattering from Cerium under pressure. Physica B+C 86-88, 41-42.

SKRIVER, H.L. (1977). Energy bands and Fermi surface for β'-MgHg and β'-MgTl. Phys. Rev. B15, 1894-1905.

STAUN OLSEN, J., BURAS, B., JENSEN, T., ALSTRUP, O., GERWARD, L., and SELSMARK, B. (1977). Influence of polarisation of the incident beam on integrated intensities in X-ray energy-dispersive diffractometry. Physics Laboratory II, University of Copenhagen, Monograph No. 77-10, 10 pp.

STEINER, M. and KJEMS, J.K. (1977). Spin waves in $CsNiF_3$ with an applied magnetic field. J. Phys. C: Solid State Phys. 10, 2665-2671.

SØRENSEN, H. (1977). Secondary electron emission from solid hydrogen and deuterium resulting from incidence of keV electrons and hydrogen ions. J. Appl. Phys. 48, 2244.

SØRENSEN, H. (1977). Energy reflection from Nb, Ag, and Au bombarded with 1-10 keV protons, Proceedings of the International Conference on Plasma Wall Interaction, Jülich 1976, Eur 578e, (Pergamon Press), Oxford, 437-442.

SZPUNAR, B. and LINDGÅRD, P.-A. (1977). Theory of temperature dependence of the magnetization in rare-earth-transition metal alloys. Phys.Stat.Sol. (b) 82, 449-456.

TAUB, H., CARNEIRO, K., KJEMS, J.K., PASSELL, L., and McTAGUE, J.P. (1977). Neutron scattering study of ^{36}Ar monolayer films adsorbed on graphite. Phys. Rev. B16, 4551-4568.

TCHEN, C.M., PECSELI, H.L., and LARSEN, S.E. (1977). Strong turbulence in magnetized plasmas. Risø Report No. 365, 26 pp.

YSSING HANSEN, F. and CARNEIRO, K. (1977). A procedure to obtain reliable pair distribution functions of non-crystalline materials from diffraction data. Nucl. Instr. Methods. 143, 569-575.

5.3 Conference contributions

BURAS, B., Combination of synchrotron radiation with the energy-dispersive method for the study of crystalline and amorphous substances. Deutsche Physikalische Gesellschaft, spring meeting, Münster, F.R.G., March 7-12.

BURAS, B., Synchrotron radiation as an X-ray source for crystallographic studies. 14th Danish Crystallography Meeting, Copenhagen, May 26-27.

BURAS, B. and NIIMURA, N., Critical point of the γ-α phase transition in Cerium,studies using neutron diffraction. Danish Physical Society, Spring Meeting, Elsinore, May 4-5.

BURAS, B., NIIMURA, N., and LEBECH, B., Critical point of the γ-α phase transition in Cerium studies using neutron diffraction. 4th European Crystallographic Meeting, Oxford, U.K., August 30 - September 3.

BURAS, B., STAUN OLSEN, J., and GERWARD, L., White beam, X-ray energy-dispersive diffractometry using synchrotron radiation. International Conference on Synchrotron Instrumentation and Developments, Orsay, France, September 12-14.

BURAS, B., STAUN OLSEN, J., GERWARD, L., HINZE, E., and WILL, G. X-ray energy-dispersive diffractometry using synchrotron radiation. Danish Physical Society, Spring Meeting, Elsinore, May 4-5.

BURAS, B., STAUN OLSEN, J., GERWARD, L., WILL, G., and HINZE, E., X-ray energy-dispersive diffractometry using synchrotron radiation. 4th European Crystallographic Meeting, Oxford, U.K., August 30 - September 3.

CARNEIRO, K., Recent resistivity and neutron scattering results from some one-dimensional conductors. Symposium on One-Dimensional Conductors, Trieste, Italy, August 10-11.

CARNEIRO, K., Neutron scattering from ^{36}Ar and ^{4}He films. International Conference on Two-Dimensional Adsorbed Phases, Marseille, France, September 6-9.

CARNEIRO, K., MACKENZIE, G.A., and WILLIAMS, J.M., Elastic constants of the one-dimensional conductor $K_2\ Pt(CN)_4\ Br_{0.3} \times H_2O$ (KCP). Danish Physical Society, Spring Meeting, Elsinore, May 4-5.

CHANG, C.T., Preliminary considerations regarding the effect of α-particles on a refuelling pellet. 8th European Conference on Controlled Fusion and Plasma Physics, Prague, Czechoslovakia, September 19-23.

CHANG, C.T., On the use of Langmuir probes in a laser produced plasma. 13th International Conference on Phenomena in Ionized Gases, Berlin, G.D.R., September 12-17.

CHRISTENSEN, O. and FRANDSEN, S., A field study of cross wind excitation of steel chimneys. International Research Seminar on Safety of Structures under Dynamic Loading, Trondheim, Norway, June 23 - July 1.

COOKE, J.F. and LINDGÅRD, P.-A., Canonical transform theory of spin waves in strongly anisotropic magnets. 23rd Annual Conference on Magnetism and Magnetic Materials. Minneapolis, Minnesota, USA, November 8-11.

DYSTHE, K.B. and PÉCSELI, H.L., Nonlinear Langmuir wave modulation. Plasma og Gasutladningssymposiet, Gausdal, Norway, February 2-5.

HINZE, E., WILL, G., BURAS, B., STAUN OLSEN, J., and GERWARD, L., Beugungsexperimente an Kristallen mit Synchrotronstrahlung. (Scattering experiments on crystals by means of synchrotron radiation). Deutsche Physikalische Gesellschaft, Spring Meeting, Münster, F.R.G., March 7-12.

HOUMANN, J.G., LEBECH, B., JENSEN, J., MACKINTOSH, A.R., McMASTERS, O.D., and GSCHNEIDNER, K.A. Jr., Impurity modes and magnetic ordering in praseodymium alloys. Danish Physical Society, Spring Meeting, Elsinore, May 4-5.

JENSEN, N.O.,Er vor viden om det atmosfæriske grænselag tilstrækkelig til almindelige ingeniørmæssige anvendelser. (Is our knowledge about the atmospheric boundary layer sufficient for normal engineering purposes?). Conference on "Klimatmätningar och klimatdata för forskningsändamål", Gävle, Sweden, October 25-27.

JENSEN, V.O., Some elements of plasma physics. Danish Physical Society, Spring Meeting, Elsinore, May 4-5.

JENSEN, V.O., Energy transfer between potential energy and ion acoustic waves. Third International Congress on Waves and Instabilities in Plasmas, Paris, France, June 27 - July 1.

JUUL RASMUSSEN, J., Electron plasma waves in a plasma filled waveguide. Plasma- og Gasutladningssymposiet. Gausdal, Norway, February 2-5.

KJEMS, J.K., The cooperative Jahn-Teller effect studied by neutron scattering. NATO Advanced Study Institute, Geilo, Norway, April 13-24.

KJEMS, J.K. and MØLLENBACH, K., The order parameter in cooperative Jahn-Teller phase transitions studied by gamma-diffraction. Danish Physical Society, Spring Meeting, Elsinore, May 4-5.

KOFOED-HANSEN, O., Recent developments in high energy physics. Danish Physical Society, Annual Meeting, November 11.

LEBECH, B. and HANSEN, P.Å. Magnetic structures and phase transitions of Neodymium single crystals. Fourth European Crystallographic Meeting, Oxford, U.K., August 30 - September 3.

LENSCHOW, D., JENSEN, N.O., MAHRT, L., and STEPHENS, P., On the structure of convective elements as observed during AMTEX. The Third General Scientific Assembly of the International Association of Geomagnetism and Aeronomy and the Second

Special Assembly of the International Association of Meteorology and Atmospheric Physics. University of Washington, Seattle, USA, August 22 - September 3.

LINDGÅRD, P.-A., Excitations and spin waves, Conference on Rare Earths and Actinides. Durham, U.K., July 4-6.

LINDGÅRD, P.-A. and SZPUNAR, B., CPA calculation of moments and transition temperatures of rare earth and rare earth-transition metal alloys. Danish Physical Society, Spring Meeting, Elsinore, May 4-5.

LINDGÅRD, P.-A. and SZPUNAR, B., CPA calculation of moments and transition temperatures of rare earth and rare earth-transition metal alloys. Conference on Rare Earths and Actinides. Durham, U.K., July 4-6.

LINDGÅRD, P.-A. and SZPUNAR, B., CPA calculation of moments and transition temperatures of rare earth and rare earth-transition metal alloys. International Conference on Magnetic Alloys and Oxides, Haifa, Israel, August 15-18.

MICHELSEN, P., PÉCSELI, H.L., and JUUL RASMUSSEN, J., Ion beam-excited, electrostatic ion cyclotron instability. Danish Physical Society, Spring Meeting, Elsinore, May 4-5.

MICHELSEN, P., PÉCSELI, H.L., and JUUL RASMUSSEN, J., Temperature effects on the ion-beam-driven electrostatic ion cyclotron instability. Third International Congress on Waves and Instabilities in Plasmas, Paris, France, June 27 - July 1.

MICHELSEN, P., PÉCSELI, H.L., and JUUL RASMUSSEN, J., Ion acoustic waves in the presence of electron plasma waves. Third International Congress on Waves and Instabilities in Plasmas, Paris, France, June 27 - July 1.

MICHELSEN, P., PÉCSELI, H.L., and JUUL RASMUSSEN, J., Ion-beam-excited ion cyclotron instability. 13th International Conference on Phenomena in Ionized Gases, Berlin, G.D.R., September 12-17.

MØLLENBACH, K., KJEMS, J.K., ALS-NIELSEN, J., and LAURSEN, I., Small-angle neutron scattering from magnetic domains in $LiTbF_4$. Danish Physical Society, Spring Meeting, Elsinore, May 4-5.

MØLLENBACH, K., KJEMS, J.K., and SMITH, S.H., Gamma-ray diffraction studies of the mosaic distribution in $TmAsO_4$ near the cooperative Jahn-Teller transition at 6 K. NATO Advanced Study Institute, Geilo, Norway, April 13-24.

NIELSEN, M., Adsorbed layers on grafoil studied by neutron scattering. Danish Physical Society, Topical Meeting on Surfaces, Århus, November 23.

NIELSEN, M., ELLENSON, W.D., and McTAGUE, J.P., The Dynamics and the Structures of Adsorbed Surfaces. International Symposium on Neutron Inelastic Scattering. Vienna, Austria, October 17-21.

NIELSEN, M., ELLENSON, W.D., and SILVERA, I., Experiments with hydrogen on grafoil and alumina. International Quantum Crystals Conference, Colorado State University, Colorado, USA, August 8-12.

NIELSEN, M., McTAGUE, J.P., and ELLENSON, W.D., Adsorbed layers of D_2, H_2, O_2 and ^3He on graphite studied by neutron scattering. International Conference on Two-Dimensional Adsorbed Phases, Marseille, France, September 6-9.

NIELSEN, M. and SILVERA, J., H_2 adsorbed on alumina, studied by neutron scattering. Danish Physical Society, Spring Meeting, Elsinore, May 4-5.

NIELSEN, P., The Danish fokamak experiment. Plasma- og Gasutladningssymposiet, Gausdal, Norway, February 2-5.

NIELSEN, P., A He-Ne laser interferrometer for Tokamak electron density measurements. 19th Annual Meeting of the Division of Plasma Physics, Atlanta, Georgia, USA, November 7-11.

OTT, H.R., KJEMS, J.K., and ANDRÉS, K., Crystal Field transitions in $PrCu_2$ near the cooperative Jahn-Teller transition at T_D = 8 K. Conference on Rare Earth Metals and Actinides, Durham, U.K., July 4-8.

PETERSEN, E.L. and LARSEN, S.E., Stochastic model building for discrete time series applied on a paleo temperature series from the last 700 000 years. Fifth Conference on Probability and Statistics in Atmospheric Sciences, Las Vegas, Nevada, USA, November 15-18.

PETERSEN, E.L., De meteorologiske beregninger i Barsebäck-rapporten. (Meteorological calculations in the Barsebäck report). Seminar on "spredningsmodellers användning på luftvårdsproblem i Norden", Norrköping, Sweden, November 1-2.

SCHOU, J. and SIGMUND, P., Secondary electron emission from electron and ion incidence on solids. Meeting on Multiple Atomic Collision Phenomena, Copenhagen, December 9-10.

SKRIVER, H.L. and ANDERSEN, O.K., Self-consistent calculation of ground-state properties for ordered transition meta' alloys.

International Conference on Physics of Transition Metals, Toronto, Canada, August 15-19.

SØRENSEN, H. and SCHOU, J., Interaction between solid nitrogen and 1-3 keV electrons. Meeting on Multiple Atomic Collision Phenomena, Copenhagen, December 9-10.

TCHEN, C.M., PÉCSELI, H.L., and LARSEN, S.E., Strong turbulence in plasmas. Plasma og Gasutladningssymposiet, Gausdal, Norway, February 2-5.

TCHEN, C.M., PÉCSELI, H.L., and LARSEN, S.E., Strong turbulence in magnetized plasmas. Third International Congress on Waves and Instabilities in Plasmas, Paris, France, June 27 - July 1.

5.4 Degrees, students, etc

V.O. Jensen defended a dissertation entitled "Some Investigations of the Ion Acoustic Wave Problem in Collisionless Plasmas" (Risø Report No. 322) on January 7, 1977, at the University of Aarhus.

The following were awarded the degree of lic.techn. (Ph.D.) for work carried out in the department:

Ian Utke Heilmann+ (Solid State Physics)
Jens Juul Rasmussen (Plasma Physics)

The following postgraduates carried out research (which will lead to the degrees of lic. tech. or lic. scient.) at the department:

Kurt Clausen	(Solid State Physics)
Sven-Erik Gryning	(Meteorology)
Jens-Peter Hansen	(Plasma Physics)
Jørgen Højstrup	(Meteorology)
Palle Buus Jensen	(Plasma Physics)
Knud Møllenbach	(Solid State Physics)
Jørgen Schou	(Plasma Physics)
Ib Troen	(Meteorology)

+ Supported by the University of Copenhagen

The following students from the Technical University of Denmark and the University of Copenhagen worked on Master's thesis projects

Kurt Clausen	(Solid State Physics)
Jens-Peter Hansen	(Plasma Physics)
Peer Herbsleb	(Plasma Physics)
Palle Buus-Jensen	(Plasma Physics)
Thorkil Jensen	(Plasma Physics)
Olaf Mathiassen	(Meteorology)
Torben Mikkelsen	(Plasma Physics)

During February and September students from th. Universities of Aarhus and Copenhagen participated in the following laboratory courses:

1) Neutron Scattering, organized by:
   J.G. Houmann, K. Møllenbach, and K. Clausen

2) Plasma Physics, organized by:
   P. Michelsen, H.L. Pécseli, and J. Juul Rasmussen

Four students from the University of Copenhagen performed measurements at DR3 as part of their training.

One foreign student sponsored by the IAESTE carried out practical work at the department as part of his general training.

6. STAFF OF THE PHYSICS DEPARTMENT

Head: Hans Bjerrum Møller

Office staff: Gerda Stauning, Grethe Sørensen, Alice Thomsen, and temporary assistants.

The sections:
6.1 Solid State Physics
6.2 Plasma Physics
6.3 Meteorology
6.4 Liquid N_2 and He Plant

6.1 Solid State Physics

Scientific staff	Technical staff
Jens Als-Nielsen*	Bjarne Breiting
Ove W. Dietrich**	Kaj Christensen
Jens Gylden Houmann**	Arent Hansen***
Jørgen Kjems	Bent Heiden
Bente Lebech	John Z. Jensen
Per-Anker Lindgård	Louis G. Jensen
Hans Bjerrum Møller	Steen Jørgensen
Mourits Nielsen	Werner Kofoed
Hans L. Skriver	Jens Linderholm
	Jørgen Munck
	Allan Thuesen
	Bent Villumsen (until July 31)

---

* On leave at Massachusetts Institute of Technology, Boston, USA, until June 30

** Moved to Energy System Studies on August 1

*** Moved to Meteorology on September 1

Consultants	Postgraduates
Ole Krogh Andersen[+]	Kurt Clausen
Bronislaw Buras[++]	Ian Utke Heilmann[+++] (until Sept. 30)
Kim Carneiro[++]	Knud Møllenbach
Allan R. Mackintosh[++]	

Long-term visitors

John Axe	Brookhaven National Laboratory, New York,USA
Gordon Mackenzie	University of Edinburgh, Scotland
Nobuo Niimura	Tohoku University, Sendai, Japan
Robert W. Youngblood	Brookhaven National Laboratory, New York,USA

Short-term visitors

W.J.L. Buyers	Chalk River Nuclear Laboratories, Canada
M. Brooks	Euratom, Karlsruhe, F.R.G.
M. Dacarogna	University of Geneva, Switzerland
W. Daniels	University of Delaware, Delaware, USA
M. Dickens	AERE Harwell, U.K.
W.D. Ellenson	Brookhaven National Laboratory, New York,USA
H. Fogedby	Institute Laue-Langevin, Grenoble, France
R.J. Elliott	Oxford University, U.K.
W. Hayes	Oxford University, U.K.
M.T. Hutchings	AERE Harwell, U.K.
G.H. Lander	Argonne National Laboratory, Illinois, USA
D.P. Landau	University of Georgia, Georgia, USA
J.P. McTague	University of California, Los Angeles, California, USA
G.S. Pawley	University of Edinburgh, Scotland
E. Rastelli	Istituto di Fisica, Milano, Italy
M. Steiner	Hahn-Meitner Institute, Berlin, F.R.G.
C. Vettier	CNRS, Grenoble, France

+ Technical University of Denmark

++ University of Copenhagen

+++ Supported by the University of Copenhagen

6.2 Plasma Physics

Scientific staff

Verner Andersen
Che-Tyan Chang
Vagn C. Jensen
Thorkil Jensen§
Leif W. Jørgensen§
Otto Kofoed-Hansen*
Poul Michelsen
Per Nielsen
Hans Pécseli
Alfred H. Sillesen (until Sept. 30)
Hans Sørensen

Technical staff

Paul Andersen
Bengt Hurup Hansen
Mogens Nielsen
Arne Nordskov
John Petersen
Børge Reher
Hans Skovgård

Consultants

Chan Mou Tchen**

Postgraduates

Jens-Peter Hansen
Palle Buus Jensen
Jørgen Schou

Long-term visitors

Valery Turikov	People's Friendship University, Moscow, USSR

Short-term visitors

A. Kildal	University of Oslo, Norway
K. Saeki	Tohoku University, Sendai, Japan
R. Schrittwieser	University of Innsbruck, Austria

---

* Also at Niels Bohr Institute, Copenhagen

**City University of New York, USA

§ Temporary assistant

6.3 Meteorology

Scientific staff	Technical staff
Niels E. Busch (until Feb. 28)	Jørgen Christensen
Carl Jørgen Christensen	Flemming Schiødt Dalsgård§
Sten Frandsen	Gunner Dalsgård
Niels Otto Jensen (from Sept. 26)	Morten Frederiksen
Leif Kristensen*	Arent Hansen (from Sept. 1)
Søren E. Larsen**	Finn Hansen
Erik Lundtang Petersen	Gunnar Jensen
	Ola Persson§
	Knud Sørensen

Consultants	Postgraduates
Chan Mou Tchen+	Sven-Erik Gryning
Ole Christensen++	Jørgen Højstrup
	Ib Troen

Long-term visitors

Dennis Thomson	Pennsylvania State University, Pennsylvania,USA

Short-term visitors

L. Mahrt	Oregon State University, Oregon, USA
J. Normann	Pennsylvania State University, Pennsylvania,USA
H.A. Panofsky	Pennsylvania State University, Pennsylvania,USA
E.W. Peterson	Oregon State University, Oregon, USA
R.B. Smith	Yale University, Connecticut, USA
P. Taylor	University of Southampton, U.K.

---

* On leave at Pennsylvania State University, USA

** On leave at University of Washington, USA, until October 5

\+ City University of New York, USA

++ ISVA, Technical University of Denmark

§ Temporary assistant

6.4 Liquid N_2 and He Plant

Technical staff

Bent Heiden
John Z. Jensen
Erik Knudsen (until June 15)

ISBN 87-550-0513-6
ISSN 0418-6443